Accepted Manuscript

Effect of hemin, baicalein and heme oxygenase-1 (HO-1) enzyme activity inhibitors on cd-induced accumulation of HO-1, HSPs and aggresome-like structures in Xenopus kidney epithelial cells

James H. Campbell, John J. Heikkila

PII: S1532-0456(18)30054-1
DOI: doi:10.1016/j.cbpc.2018.04.003
Reference: CBC 8411

To appear in:

Received date: 29 March 2018
Revised date: 20 April 2018
Accepted date: 20 April 2018

Please cite this article as: James H. Campbell, John J. Heikkila , Effect of hemin, baicalein and heme oxygenase-1 (HO-1) enzyme activity inhibitors on cd-induced accumulation of HO-1, HSPs and aggresome-like structures in Xenopus kidney epithelial cells. The address for the corresponding author was captured as affiliation for all authors. Please check if appropriate. Cbc(2018), doi:10.1016/j.cbpc.2018.04.003

Revised MS 28535

Effect of hemin, baicalein and heme oxygenase-1 (HO-1) enzyme activity inhibitors on Cd-induced accumulation of HO-1, HSPs and aggresome-like structures in *Xenopus* kidney epithelial cells

James H. Campbell and John J. Heikkila

Department of Biology, University of Waterloo

Waterloo, ON

Canada N2L 3G1

***Corresponding author:**
Dr. John J. Heikkila
Department of Biology,
University of Waterloo,
Waterloo, ON
Canada N2L 3G1
Tel: 519-888-4567 Ext. 33076
FAX: 519-746-0614
heikkila@uwaterloo.ca

Running Title: Effect of cadmium on HO-1 and HSP accumulation and function in *Xenopus* cells

Abstract

Cadmium is a highly toxic environmental pollutant that can cause many adverse effects including cancer, neurological disease and kidney damage. Aquatic amphibians are particularly susceptible to this toxicant as it was shown to cause developmental abnormalities and genotoxic effects. In mammalian cells, the accumulation of heme oxygenase-1 (HO-1), which catalyzes the breakdown of heme into CO, free iron and biliverdin, was reported to protect cells against potentially lethal concentrations of $CdCl_2$. In the present study, $CdCl_2$ treatment of A6 kidney epithelial cells, derived from the frog, *Xenopus laevis*, induced the accumulation of HO-1, heat shock protein 70 (HSP70) and HSP30 as well as an increase in the production of aggregated protein and aggresome-like structures. Treatment of cells with inhibitors of HO-1 enzyme activity, tin protoporphyrin (SnPP) and zinc protoporphyrin (ZnPP), enhanced $CdCl_2$-induced actin cytoskeletal disorganization and the accumulation of HO-1, HSP70, aggregated protein and aggresome-like structures. Treatment of cells with hemin and baicalein, which were previously shown to provide cytoprotection against various stresses, induced HO-1 accumulation in a concentration-dependent manner. Also, treatment of cells with hemin and baicalein suppressed $CdCl_2$-induced actin dysregulation and the accumulation of aggregated protein and aggresome-like structures. This cytoprotective effect was inhibited by SnPP. These results suggest that HO-1-mediated protection against $CdCl_2$ toxicity includes the maintenance of actin cytoskeletal and microtubular structure and the suppression of aggregated protein and aggresome-like structures.

Key Words: HO-1, cadmium, aggregated protein, aggresomes, HSP70, HSP30, immunocytochemistry, cytoskeleton, SnPP, ZnPP

1. Introduction

Cadmium is a carcinogenic and toxic metal that occurs naturally in the environment or as a result of industrial pollution (Waisberg et al., 2003; Joseph, 2009; Templeton and Liu, 2010). Continuous exposure to cadmium has been associated with a number of disease states including Alzheimer's disease and lung cancer (Mendez-Armenta and Rios, 2007; Nordberg, 2009; Johri et al., 2010; Templeton and Liu, 2010). While many organs and tissues are adversely affected by cadmium, the kidney is particularly sensitive to its toxic effects (Waisberg, 2003; Nordberg, 2009; Johri et al., 2010). Cadmium exposure can result in a number of harmful intracellular effects including the production of reactive oxygen species (ROS), damage to DNA and its repair system and the formation of denatured and abnormal proteins, which can become aggregated and form aggresome-like structures (Waisberg et al., 2003; Bertin and Averbeck, 2006; Mouchet et al., 2006; Mendez-Armenta and Rios, 2007; Khan et al., 2015). Also cadmium exposure can induce the expression of a number of genes which are thought to be involved in counteracting its injurious effects including those encoding heme oxygenase-1 (HO-1) and heat shock proteins (HSPs; Alam et al., 2000; Ovelgonne et al., 1995; Somji et al., 2000; Music et al., 2014).

HO-1, which is the stress-inducible isozyme of heme oxygenase, catalyzes the breakdown of heme into CO, free iron and biliverdin (Platt and Nath, 1998; Hwang et al., 2009). While HO-1 is an ER protein, it lacks a signal peptide and a KDEL retention sequence (Gottlieb et al., 2012). However, HO-1 is posttranslationally inserted into the ER membrane via its C-terminal end (Yoshida and Sato, 1989; Gottlieb et al., 2012). Cadmium-induced HO-1 accumulation has been reported in a number of organisms

including mouse, zebrafish, carp, and chicken (Sardana et al., 1982; Alam et al., 2000; Blechinger et al., 2007; Jancsó and Hermesz, 2015). Other agents were found to induce HO-1 accumulation in mammalian cultured cells including hemin and the plant flavonoid, baicalein (Alam et al., 2000; Brouard et al., 2000; Li-Weber, 2009). Cadmium-, hemin- and baicalein-induced *ho-1* gene expression involves the Maf recognition elements (MARE)/ nuclear factor-erythroid 2 family member (Nrf2) pathway (Alam et al., 2000; Alam and Cook, 2007; Macleod et al., 2009). It has been proposed that cadmium-induced *ho-1* gene expression may include the cadmium response element (CdRE) and the transcription factors HSF1 and pescadillo (Sikorski et al., 2006; Koizumi et al., 2007).

A number of studies in mammalian systems examined the cytoprotective nature of HO-1 accumulation (Brouard et al., 2000; Lang et. al., 2004). For example, pretreatment of rats with hemin, which upregulated HO-1 levels, protected their kidneys and testes against damage by mercury and cadmium, respectively (Yoneya et al., 2000; Fouad et al., 2009). Baicalein-induced HO-1 accumulation was associated with protection against vascular injuries and enhanced survival of human cardiomyocytes in response to oxidative challenges (Chen et al., 2006; Cui et al., 2015). HO-1-mediated cytoprotection against oxidative stress involves its catalytic breakdown products, CO and bilirubin (Gozzelino et al., 2010; Correa-Costa et al., 2012). For example, HO-1-mediated production of CO inhibited apoptosis through its interaction with p38 mitogen-activated kinase (MAPK; Brouard et al., 2000). Also, bilirubin, a potent antioxidant, protected HeLa cells and cultured rat neurons against H_2O_2-mediated necrotic cell death (Stocker et al., 1987; Morita et al., 1997; Doré et al., 1999; Baranano et al., 2002). HO-1-induced

cytoprotection against a variety of stressors was reported to be suppressed in a competitive fashion by the HO-1 enzyme activity inhibitors and heme analogs, tin protoporphyrin (SnPP) and zinc protoporphyrin (ZnPP; Srisook et al., 2005; Varga et al., 2007; Miyake et al., 2010; Wong et al., 2011). The addition of SnPP was found to sensitize mouse T cells to hypoxia by inhibiting HO-1 enzyme activity while ZnPP supressed HO-1-mediated protection against cadmium stress in rat glial cells (Srisook et al., 2005; Dey et al., 2014).

Cadmium has been shown to induce the accumulation of HSPs in a wide range of organisms (Heikkila et al., 1982; Ovelgonne et al., 1995; Somji et al., 2000; Blechinger et al., 2007; Woolfson and Heikkila, 2009; Selim et al., 2012). HSPs are molecular chaperones that were classified primarily by size into families including small HSPs, HSP40, HSP60, HSP70, and HSP90 (Morimoto, 2008). Some HSPs are strictly stress-inducible while others are constitutively expressed or constitutive but responsive to induction. HSPs perform a number of roles in maintaining cellular protein homeostasis, such as protein folding, preventing aggregation of unfolded proteins and protein translocation (Balch et al., 2008). The heat shock response (HSR) involves the transcription of *hsp* genes to counteract stresses that affect cellular protein homeostasis such as high temperature, heavy metals or elevated levels of ROS (Heikkila, 2004; Voellmy, 2004; Morimoto, 2008; Heikkila, 2010). Under non-stress conditions, monomeric heat shock factor-1 (HSF-1) is functionally inactive as it is in a complex with HSP90 (Voellmy, 2004; Morimoto, 2008). Stress-induced accumulation of unfolded/misfolded protein results in the dissociation of HSP90 from HSF-1, which then trimerizes, undergoes phosphorylation, translocates to the nucleus, binds to the heat

shock element (HSE) and stimulates the transcription of *hsp* genes (Voellmy 2004; Morimoto 2008). Cadmium treatment of cells, which was found to cause protein damage due to oxidative stress or the formation of polydentate coordination complexes with the protein backbone resulted in the accumulation of misfolded/damaged protein leading to the activation of the HSR (Bharadwaj et al., 1998; Waisberg et al., 2003; Morimoto, 2008; Galazyn-Sidorczuk et al., 2009; Tamás et al., 2014).

Aquatic poikilotherms, such as amphibians and fish, are susceptible to the effects of cadmium as it can enter dermally through the skin and gills in a concentration-dependent manner by diffusion or active ion transport (Faurskov and Bjerregaard, 2002). During early stages of embryogenesis of the frog, *Xenopus laevis*, cadmium was determined to be especially toxic (Mouchet et al., 2006). Also, treatment of *X. laevis* A6 kidney epithelial cells with $CdCl_2$ induced the accumulation of HO-1 and HSPs, including HSP70, HSP30, immunoglobulin-binding protein (BiP), and HSP110, as well as inhibition of the ubiquitin proteasome system (UPS) and the formation of aggresome-like inclusion bodies (Voyer and Heikkila, 2008; Woolfson and Heikkila, 2009; Brunt et al., 2012; Khamis and Heikkila, 2013; Music et al., 2014; Khan et al., 2015; Heikkila, 2017; Shirriff and Heikkila, 2017). When the amount of aggregated or unfolded protein exceeds the capacity of the UPS machinery to degrade it, the cell transports protein aggregates along microtubules using dynein motors to form aggresomes proximal to the nucleus (Taylor et al, 2003; An and Statsyuk, 2015). Aggresomes, which are sequestered protein aggregates within a vimentin cage, minimize the toxic effects of cellular protein aggregates until their proteolysis by autophagy (Bolhuis and Richter-Landsberg, 2010; An and Statsyuk, 2015). A variety of HSPs including HSP70, HSP40 and sHSPs were

reported to associate with aggresomes and aggresome-like structures, suggesting a role for HSPs in their formation (Tyedmers et al., 2010; Katoh et al., 2004; Bolhuis and Richter-Landsberg, 2010). Recently, it was reported that $CdCl_2$ treatment of *Xenopus* A6 cells caused a co-localization of HSP30 with aggresome-like structures (Khan et al., 2015).

Given that $CdCl_2$ treatment of *X. laevis* A6 cells induced the accumulation of HO-1, HSPs, aggregated protein and the formation of aggresome-like structures and disorganization of the actin cytoskeleton, we were interested in determining whether modification of HO-1 enzyme activity could modulate these responses. Initially, we investigated the effect of HO-1 enzyme activity inhibitors SnPP and ZnPP on HSP70 and HO-1 accumulation and the effect of SnPP on $CdCl_2$-induced production of aggregated protein and aggresome-like structures. In the next phase of this research, we examined the effects of treating A6 cells with the HO-1 accumulation inducers, hemin and baicalein, prior to the addition of $CdCl_2$ to determine whether this treatment regimen could ameliorate the toxic effects of this metal. In these latter studies, the actin cytoskeleton, microtubular structure and the formation of aggregated protein and aggresome-like structures were examined.

2.0 Materials and methods

2.1 Chemicals

$CdCl_2$ (Bioshop, Burlington, ON) was prepared as a 100 mM stock solution in sterile water (Sigma-Aldrich). Hemin (Sigma-Aldrich, Oakville, ON) was prepared by dissolving it in dimethyl sulfoxide (DMSO; Sigma-Aldrich) to yield a 1.5 mM stock solution. HO-1 enzyme activity inhibitors, tin protoporphyrin (SnPP; Enzo Life Sciences, Farmingdale, NY) and zinc protoporphyrin (ZnPP; Enzo Life Sciences) were dissolved in DMSO to produce 1.5 mM stock solutions. Baicalein (Sigma-Aldrich) was also dissolved in DMSO to produce a 10 mM stock solution. After stocks were made, hemin, ZnPP, SnPP and baicalein were kept wrapped in tin foil to protect them from light prior to storage at -20 °C.

2.2 Culture of X. laevis A6 kidney epithelial cells

X. laevis A6 kidney epithelial cells were obtained from the American Type Culture Collection (CCL-102; Rockville, MD). Cells were cultured in T75 cm^2 flasks (VWR, Mississauga, ON) at 22 ºC using 70% L15 (Leibowitz) cell culture media with 10% fetal bovine serum and 1% penicillin/streptomycin (Sigma-Aldrich). Once the cells were confluent, they were rinsed once with 1 ml versene [0.02% (w/v) KCl, (0.8% (w/v) NaCl, 0.02% (w/v) KH_2PO_4, 0.115% (w/v) $NaHPO_4$, 0.02% (w/v) Na_2EDTA] and then again with 2 ml versene followed by treatment with 1 ml of 1X trypsin (Sigma-Aldrich) in Hank's balanced salt solution (HBSS, Sigma-Aldrich) to facilitate cell detachment. Fresh media was then added to resuspend cells and inactivate trypsin followed by transfer of cells to new flasks.

2.3 Cell treatments

Chemical treatments were administered to cells at 80-90% confluency. In experiments using 25 to 275 µM $CdCl_2$, 10 to 30 µM hemin or 50 to 400 µM baicalein, these chemicals were mixed with L-15 media and administered to the cells at the final concentration described. In experiments examining HO-1 enzyme activity inhibitor effects on cadmium-treated cells, cells were treated with ZnPP or SnPP for 4 h prior to supplementation with $CdCl_2$ for 16 h at 22 °C. Finally, cytoprotection studies involved the incubation of cells with baicalein or hemin and/or SnPP for 4 h prior to supplementation with $CdCl_2$ for 16 h, followed by a 4 h recovery in fresh media.

2.4 Protein isolation and quantification

Prior to collection, cells were rinsed once with 2 ml of 65% HBSS and then resuspended in 1 ml 100% HBSS. Cells were transferred to 1.5 ml microcentrifuge tubes (Eppendorf centrifuge; Model No. 5810R; Mississauga, ON) and collected by centrifugation at 14,000 rpm for 1 min and then stored at -80 °C. For protein isolation, cells were lysed using 300 µL of 1% SDS lysis buffer (200 mM sucrose, 2 mM EGTA, 1 mM EDTA, 40 mM NaCl, 30 mM HEPES, pH 7.4, 1% protease inhibitor and 1% SDS) followed by sonication on ice with a sonic dismembranator (Model 100, Fisher Scientific; Waltham, MA, USA). Cell debris and unlysed cells were separated from the protein isolate by centrifugation at 14,000 rpm for 60 min at 4 °C. Protein content of the supernatant was quantified by the bicinchoninic acid protein quantification assay kit (Pierce, Rockford, IL, USA). Protein standards were made by diluting a bovine serum albumin (BSA; Bioshop) solution with MilliQ water to final concentrations ranging from 0 to 2 mg/mL. Standards and samples were transferred in triplicate to a polystyrene 96-

well plate followed by the addition of the assay reagents. The plate was then incubated at 37 °C for 30 min and monitored at 562 nm using a Versamax Tunable microplate reader (Molecular Devices, Sunnyvale, CA, USA) and Softmax Pro software.

2.5 SDS-PAGE and immunoblot analysis

Protein samples were separated by sodium dodecyl-sulphate polyacrylamide gel electrophoresis (SDS-PAGE) using 12% acrylamide gels as previously described (Young and Heikkila, 2010). Protein was transferred from acrylamide gels to nitrocellulose membranes using a Trans-Blot Semi-dry transfer system (Bio-Rad, Mississauga, ON) for 25 min at 20 V. Transfer efficiency was assessed by protein staining with Ponceau S (Sigma-Aldrich). Blots were incubated for 1 h in 5% skim milk (Carnation, Markham ON) in Tris buffered saline (20 mM Tris pH 7.5, 300 mM NaCl) with 0.1% Tween-20 (TBS-T; Sigma-Aldrich) to inhibit non-specific protein binding. The membranes were incubated with rabbit anti-HO-1 (1:500; Enzo Life Sciences; Catalog no. BML-HC3001-100), anti-*Xenopus* HSP70 (1:350; Gauley et al., 2008), anti-*Xenopus* HSP30 (1:500; Fernando and Heikkila, 2000), or anti-actin (1:200; Sigma; Catalog no. A2066) polyclonal antibodies diluted in 5% skim milk solution and left overnight. Membranes were then washed with TBS-T once for 15 min and then twice for 10 min each followed by incubation with alkaline phosphatase-conjugated goat-anti-rabbit IgG antibodies (BioRad) in TBS-T with 5% blocking for 1 h at 22 °C. Membranes were rinsed with TBS-T for 15 min followed by two 5 min rinses. Bands were then visualized by incubating blots in alkaline phosphatase detection buffer (100 mM Tris pH 9.5, 100 mM NaCl, 50 mM $MgCl_2$) with 0.3% nitro blue tetrazolium (Roche) and 0.17% 5-bromo-4-chloro-3-idolyl phosphate toluidine salt (Roche).

2.6 Densitometry

Densitometric analysis of immunoblots was performed, within the range of linearity, using Image J software (Version 1.49; National Institute of Health; http://rsb.info.nih.gov/ij/) to quantify band intensity. The band intensity of each sample was expressed as a percentage of the maximum value for HO-1, HSP70, or HSP30 in a particular trial. The percentages for a given treatment were averaged across three replicates and graphed. Standard error of the mean was indicated as vertical error bars. Significance ($p < 0.05\%$) between control and treatment intensity was determined using one-way ANOVA with Tukey's post hoc test.

2.7 Immunocytochemistry and laser scanning confocal microscopy (LSCM)

Cells for laser scanning confocal microscopy imaging were grown on flame sterilized base-washed coverslips (VWR; Catalog no. 48366-067) in Petri dishes (VWR, Catalog no. 351029). Following various treatments (see Section 2.3), coverslips were rinsed with phosphate-buffered saline supplemented with magnesium and calcium (PBS; 1.37 M NaCl, 67 mM Na_2HPO_4, 26 mM KCl, 14.7 mM H_2PO_4, 1 mM $CaCl_2$, 0.5 mM $MgCl_2$ pH 7.4). Coverslips were then transferred to small Petri dishes and fixed with 3.7% paraformaldehyde (BDH Inc., Toronto, ON) in PBS for 15 min followed by three further washes for 5 min each and then permeabilized with 0.3% Triton X-100 (TX-100; Sigma-Aldrich) in PBS for 10 min. Coverslips were washed 3 times with PBS for 2 min each and then incubated in 3.7% BSA in PBS overnight at 4 °C. They were then incubated with dilutions of rabbit anti-HO-1, 1:500 anti-HSP30 or 1:250 anti-α-tubulin antibody (Sigma, Catalog no. T9026) in PBS w/ 3.7% BSA solution for 1 h at 22 °C. After incubation, the coverslips were washed 3 times with PBS and then incubated with a

1:2,000 dilution of fluorescent-conjugated goat anti-rabbit IgG or goat anti-mouse IgG Alexa Fluor 488 secondary antibodies (Invitrogen Molecular Probes, Carlsburg, CA) in PBS with 3.7% BSA for 30 min followed by 3 washes with PBS. For actin visualization, coverslips were incubated in PBS with 3.7% BSA containing a 1:60 dilution of rhodamine-tetramethylrhodamine-5-isothiocyanate phalloidin (TRITC; Invitrogen Molecular Probes) for 15 min in the dark. The Proteostat aggresome detection kit (Enzo Life Sciences, Plymouth Meeting, PA, USA) was used to detect the presence of aggregated protein and/or aggresome-like structures according to the manufacturer's instructions. The cover slips were dried and then mounted on glass slides using Vectashield mounting medium (Vector Laboratories, Burlingame CA) containing 4, 6-diamidino-2-phenylindole (DAPI). Slides were sealed using clear nail polish and stored at 4 °C until viewed using a Zeiss Axiovert 200 confocal microscope with LSM 510 META software (Carl Zeiss Canada Ltd., Mississauga, ON).

3.0 Results

3.1 Pattern of HO-1, HSP70, HSP30 and aggregated protein/aggresome-like structure accumulation in cells treated with $CdCl_2$

This study examined the effect of different concentrations of $CdCl_2$ on HO-1, HSP70 and HSP30 accumulation in *X. laevis* A6 cells by immunoblot and subsequent densitometric analysis. As shown in Fig. 1A, treatment of cells with 200 μM $CdCl_2$ showed the highest levels of HO-1 accumulation. Cells treated with 25, 50 or 100 μM $CdCl_2$ resulted in HO-1 levels that were 18%, 48% and 88%, respectively, of levels attained at 200 μM. Also, $CdCl_2$ treatment induced HSP30 and HSP70 accumulation at 25 μM and 100 μM $CdCl_2$, respectively, with the highest levels of both HSPs at 200 μM. Finally, the relative levels of actin remained constant in cells treated with different concentrations of $CdCl_2$. As shown in Fig. 1B and C, treatment of cells with 200 μM $CdCl_2$ resulted in the accumulation of HO-1 and HSP30 in granular patterns in the perinuclear region. Some larger HSP30 complexes were also observed in the cytoplasm near the nucleus (indicated with white arrows). HSP70 was not examined by immunocytochemistry because the affinity-purified anti-*Xenopus* HSP70 antibody, which was used successfully in immunoblot analysis, did not specifically detect HSP70 by immunocytochemistry (Gauley et al., 2008; Khan and Heikkila, 2014). $CdCl_2$ treatment resulted in disorganization of actin fibres and membrane ruffling. Finally, incubation of cells with 200 μM $CdCl_2$ resulted in some microtubule filament disorganization and the accumulation of aggregated protein primarily in the perinuclear region in a granular fashion (Fig. 1D). Large aggresome-like structures, as indicated by the white arrows, were also detected.

3.2 Effect of HO-1 enzyme activity inhibitors on $CdCl_2$-induced accumulation of HO-1, HSP70 and aggregated protein/aggresome-like structures.

Since $CdCl_2$ treatment of A6 cells enhanced the accumulation of HO-1 and HSP70, it was of interest to determine whether treatment with the HO-1 enzyme activity inhibitors, tin protoporphyrin (SnPP) and zinc protoporphyrin (ZnPP), could modify the effects of $CdCl_2$. As shown in Fig. 2, the presence of either 5 μM ZnPP or 15 μM SnPP enhanced 50 μM $CdCl_2$-induced accumulation of HO-1 compared to $CdCl_2$ alone. Densitometric analysis determined that the relative level of HO-1 found with SnPP or ZnPP was not statistically different from control levels. The HO-1 level in cells treated with 50 μM $CdCl_2$ was present at 45% of maximum levels whereas the mean relative density of SnPP and ZnPP plus $CdCl_2$ was 90% and 80%, respectively. Enhancement of $CdCl_2$-induced HO-1 accumulation was also observed using immunocytochemistry (data not shown). While the HO-1 enzyme activity inhibitors induced very low levels of HSP70 accumulation and 50 μM $CdCl_2$ induced only a slight increase in HSP70 levels relative to control, treatment with ZnPP or SnPP plus $CdCl_2$ resulted in significant increases in HSP70 accumulation.

Given that treatment of A6 cells with HO-1 enzyme activity inhibitors enhanced $CdCl_2$-induced accumulation of both HO-1 and HSP70, we examined the effect of SnPP plus $CdCl_2$ on actin cytoskeletal, microtubular structure and the presence of aggregated protein. As shown in Fig. 3, actin stress fibres and the pattern of microtubules in cells treated with SnPP or 100 μM $CdCl_2$ resembled those of control cells. In cells treated with SnPP prior to supplementation with $CdCl_2$, there was noticeable membrane ruffling and disorganization of the actin cytoskeleton while tubulin filaments appeared to be more

tangled compared to control. As indicated in Fig. 3, cells treated with 15 μM SnPP resulted in minimal accumulation of aggregated protein, as determined by Proteostat dye staining, that was similar to control cells. An increase in aggregated protein in the perinuclear region was detected in cells treated with 100 μM $CdCl_2$. However, this accumulation of aggregated protein was enhanced in cells treated with SnPP prior to supplementation with $CdCl_2$. Furthermore, these cells were characterized by the presence of larger, aggresome-like staining structures, as indicated by white arrows. Similar results were observed using ZnPP (data not shown).

3.3 Pattern of HO-1 accumulation in cells treated with hemin or baicalein

Since HO-1 enzyme activity inhibitors enhanced the levels of $CdCl_2$-induced aggregated protein and aggresome-like structures, we examined the effect of hemin and baicalein, which are known HO-1 inducers in mammalian cells, on $CdCl_2$-treated cells (Salahudeen et al., 2001; Srisook et al., 2005; Fouad et al., 2009; Gozzelino et al., 2010; Cui et al., 2015). Since the effects of hemin and baicalein on HO-1 accumulation had not been investigated in amphibians, initially we examined the effect of different concentrations of these agents on HO-1 accumulation in A6 cells by immunoblot and subsequent densitometric analysis. As shown in Fig. 4A, maximal levels of HO-1 occurred in cells incubated for 16 h with 25 μM hemin. Densitometric analysis revealed that while control cells had very low levels of HO-1, cells treated with 10, 15, 20 and 30 μM hemin displayed HO-1 levels that were 65%, 83%, 90%, and 94%, respectively, of the value obtained with 25 μM hemin (Fig. 4A). In cells treated with baicalein for 16 h, elevated levels of HO-1 were observed at 50 μM and 100 μM with peak levels at 200 μM while treatment at 400 μM resulted in a reduction to 60% of its peak value (Fig. 4B).

HSP70 and HSP30 accumulation was not detected in response to hemin or baicalein treatment (data not shown). Finally, the relative levels of actin remained constant in cells treated with different concentrations of hemin and baicalein. Also, hemin- and baicalein-induced accumulation of HO-1 in A6 cells were the result of *de novo* synthesis since pretreatment of cells with actinomycin D or cycloheximide inhibited HO-1 induction (data not shown).

3.4 Analysis of HO-1 localization in hemin- and baicalein-treated cells.

Immunocytochemical analysis was employed to examine the intracellular localization of HO-1 in response to hemin and baicalein and treatment (Fig. 5). In control cells, HO-1 was either not detectable or present at relatively low levels. Cells treated with 25 μM hemin or 200 μM baicalein showed an intense accumulation of HO-1. In response to each of these stressors, HO-1 accumulation was present in the perinuclear region in a punctate pattern with some staining in the nucleus. Actin filaments, as detected using phalloidin staining, revealed a slight disorganization in A6 cells treated with hemin or baicalein (Fig. 5). In other experiments, microtubule structure was not markedly affected by 25 μM hemin or 200 μM baicalein treatment (data not shown).

3.5 Effect of hemin and baicalein treatment on $CdCl_2$-induced HO-1 accumulation and actin cytoskeletal structure.

As mentioned previously, various studies reported that treatment of cells with hemin or baicalein have the potential to ameliorate the deleterious effects of potentially toxic conditions including $CdCl_2$ exposure (Srisook et al., 2005; Fouad et al., 2009;). Thus, we investigated the ability of low concentrations of hemin or baicalein to protect

A6 cells from a relatively high and lethal concentration of $CdCl_2$. As shown in Fig. 6 and 7, treatment of cells with 10 μM hemin or 50 μM baicalein for 16 h had no discernable effect on the actin cytoskeleton whereas exposure of cells to 275 μM $CdCl_2$ resulted in actin cytoskeletal disorganization including cell rounding, membrane ruffling and/or cytoskeletal collapse. However, treatment of cells with hemin or baicalein prior to the addition of $CdCl_2$ resulted in the presence of control-like actin stress fibres although some membrane ruffling persisted at the cell periphery. In these latter experiments, the inclusion of SnPP eliminated the cytoprotective effect against $CdCl_2$ provided by hemin or baicalein. Cells treated with SnPP prior to the addition of $CdCl_2$ showed a severe disruption of the actin cytoskeleton (data not shown). Also, elevated levels of HO-1 were observed in the perinuclear region of cells treated with hemin or baicalein prior to the addition of $CdCl_2$ in contrast to the lower levels of HO-1 found with hemin, baicalein, $CdCl_2$ or SnPP alone (Fig. 6 and 7).

3.6 Effect of hemin and baicalein treatment on $CdCl_2$-induced aggregated protein and aggresome-like structures.

In the next series of experiments, we examined the effect of treating A6 cells with hemin or baicalein prior to the addition of $CdCl_2$ on the accumulation of aggregated protein (Fig. 8 and 9). Treatment of cells with 275 μM $CdCl_2$ induced perinuclear accumulation of aggregated protein as well as the presence of large aggresome-like staining structures. However, exposure of cells to 10 μM hemin or 50 μM baicalein followed by supplementation with $CdCl_2$ resulted in diminished amounts of both diffuse and perinuclear aggregated protein and aggresome-like staining structures. When cells were treated with SnPP and hemin or baicalein prior to the addition of $CdCl_2$, aggregated

protein and aggresome-like structures were observed. In an examination of microtubule structure, treatment with 275 μM $CdCl_2$ resulted in some disorganization and intertwining of microtubules. This effect was mitigated in cells treated with hemin or baicalein prior to $CdCl_2$ addition as they had more elongated, parallel microtubules compared to $CdCl_2$ alone. In cells that were treated with SnPP and hemin prior to supplementation with $CdCl_2$, the microtubules had a mesh-like appearance.

Previously, our laboratory reported that $CdCl_2$-induced aggresome-like structures that co-localized with the small HSP, HSP30 (Khan et al., 2015). Given these earlier results, HSP30 localization was examined in the current study. As shown in Figs. 10 and 11, cells treated with $CdCl_2$ alone displayed the accumulation of HSP30 in a punctate pattern with larger staining structures, as indicated by the white arrows. These larger anti-HSP30 antibody stained structures co-localized with the aggresome-like structures (detected by the Proteostat dye) given their yellow color in the merged channel. This finding was verified by means of Z-stack analysis (data not shown). In cells treated with hemin or baicalein prior to supplementation with $CdCl_2$, the amount of aggregated protein was reduced compared to $CdCl_2$ alone whereas the amount of HSP30 accumulation in some cells was elevated and had a more diffuse pattern of cytoplasmic distribution and fewer larger structures. Addition of SnPP plus hemin or baicalein prior to $CdCl_2$ treatment resulted in cells having a pattern of HSP30 accumulation similar to $CdCl_2$ alone.

4.0 Discussion

In this study, treatment of *X. laevis* A6 cells with $CdCl_2$ induced the accumulation of HO-1, HSP70 and HSP30. Induction of HO-1 and HSPs by cadmium has been documented across a wide range of organisms including amphibians, fish, and mammals (Heikkila et al., 1982; Sardana et al., 1982; Woolfson and Heikkila, 2009; Søfteland et al., 2010; Khamis and Heikkila, 2013; Music et al., 2014; Shirriff and Heikkila, 2017). It has been suggested that $CdCl_2$-induced HO-1 accumulation involves cadmium-mediated generation of ROS and disruption of Nrf2/Keap1 association causing Nrf2 stabilization and permitting its binding to MARE and subsequent transcription of the *ho-1* gene (Alam et al., 2000; Ryter et al., 2006). Treatment of cells with $CdCl_2$ can also trigger the HSR leading to the expression of *hsp* genes due to an increase in unfolded proteins resulting from cadmium-induced oxidative damage, reaction with vicinal thiol groups or substitution for zinc in proteins (Bharadwaj et al., 1998; Waisberg et al., 2003; Voellmy, 2004; Morimoto 2008; Galazyn-Sidorczuk et al., 2009; Heikkila, 2010; Tamás et al., 2014). Interestingly, treatment of A6 cells with HO-1 enzyme activity inhibitors, SnPP and ZnPP, enhanced the levels of $CdCl_2$-induced HO-1 and HSP70. It is possible that treatment of A6 cells with SnPP or ZnPP enhanced the ROS-generating effects of $CdCl_2$. Previously it was reported that HO-1 levels and ROS production in cadmium-treated liver cells were significantly enhanced by the addition of HO-1 enzyme activity inhibitors (Lawal et al., 2015). Also, ZnPP treatment increased the oxidative stress-mediated induction of HO-1 accumulation and the cytotoxicity of the chemotherapeutic agent, gemcitabine, in human prostate cells (Varga et al., 2007). While the effect of HO-1 enzyme activity inhibitors on HSP accumulation has not been examined in other

organisms, these agents may have caused an increase in $CdCl_2$-induced protein damage or unfolding leading to a more dynamic HSR resulting in an elevated level of HSP70. Support for this latter possibility was indicated by the enhanced amounts of aggregated protein and aggresome-like structures that were detected in A6 cells treated with 100 μM $CdCl_2$ and SnPP compared to $CdCl_2$ alone.

Treatment of A6 cells with cadmium plus SnPP also induced the disorganization of the actin cytoskeleton and microtubular structure to an extent that was greater than observed with $CdCl_2$ alone. Previous studies reported that cadmium treatment caused the disruption of the actin cytoskeleton and/or the disassembly or destruction of microtubules in various cell lines including carp hepatocyte, rat renal proximal tubule and mouse 3T3 cells (Perrino and Chou, 1986; Wang et al., 1996; Nawaz et al., 2005). It was suggested in these studies that the dysregulation of the actin cytoskeleton and microtubule network may be caused, in part, by $CdCl_2$-induced oxidative stress. Treatment of mammalian cells with $CdCl_2$ or oxidative stress can cause actin fragmentation and depolymerisation (Huot et al., 1996; Wang et al., 1996). It is likely that treatment of A6 cells with SnPP/ZnPP and $CdCl_2$ caused an increase in ROS-induced damage to proteins associated with the actin cytoskeleton and microtubular network (Galazyn-Sidorczuk et al., 2009; Tamás et al., 2014).

The next phase of this research examined the effect of the HO-1 inducers, hemin and baicalein, on $CdCl_2$-treated A6 cells. Given the lack of information regarding the effects of hemin and baicalein in *Xenopus*, initial analysis examined their effect on HO-1 accumulation. In A6 cells, both hemin and baicalein induced a dose-dependent accumulation of HO-1 at concentrations that have been employed in studies with other

animal systems (Salahudeen et al., 2001; Lang et al., 2004; Chen et al., 2006; Lin et al., 2007; Zhang et al., 2012; Choi et al., 2016). The finding that actinomycin D and cycloheximide inhibited hemin- and baicalein-induced HO-1 in A6 cells indicated the involvement of *de novo* transcription and translation. In mammalian cells, it was reported that heme can bind directly to the repressor protein, Bach1, causing it to detach from the MARE site and permitting the binding of Nrf2 (Ogawa et al., 2001; Zenke-Kawasaki, 2007). Other studies suggested that baicalein directly modified cysteine residues in Keap-1 causing its disassociation from Nrf2 resulting in increased Nrf2 stabilization and subsequent *ho-1* gene expression (Zhang et al., 2012, Cui et al., 2014). In A6 cells, it is tenable that the aforementioned mechanisms are involved in hemin- and baicalein-induced accumulation of HO-1.

The finding that hemin and baicalein induced HO-1 accumulation in A6 cells in a punctate pattern with enrichment in the perinuclear region was in agreement with mammalian studies (Yoshida and Sato, 1989; Gottlieb et al., 2012). Perinuclear localization of HO-1 in *Xenopus* A6 cells was also found after treatment with $CdCl_2$, sodium arsenite, MG132 and isothiocyanates (Music et al, 2014; Khamis and Heikkila, 2018). In some A6 cells, hemin- and baicalein-induced HO-1 accumulation was found in the nucleus. Studies in mammalian cells determined that HO-1, which is anchored to the ER by a C-terminal transmembrane region such that it faced the cytosol, could be cleaved from its ER anchor and undergo translocation to the nucleus (Converso et al., 2006; Lin et al., 2007; Sacca et al., 2007; Namba et al., 2014). The punctate pattern of hemin- or baicalein-induced HO-1 accumulation in A6 cells may be the result of HO-1 oligomerization as studies in mammalian cells determined that HO-1 can form higher

order complexes containing biliverdin reductase (Huber et al., 2009; Linnenbaum et al., 2012).

Treatment of A6 cells with hemin and baicalein were able to mitigate the effects of 275 μM $CdCl_2$ on actin cytoskeletal structure. These findings suggested that the cytoprotection conferred by hemin and baicalein may have been mediated by HO-1 since the protective effects were inhibited by SnPP. In other studies, hemin-induced protection of rats against cadmium-induced testicular damage was suppressed by SnPP (Fouad et al., 2009). Also, elevated levels of HO-1 induced by NO protected rat glial cells from the toxic effects of $CdCl_2$-induced oxidative stress (Srisook et al., 2005). While the effect of baicalein-induced protection from the effect of $CdCl_2$ has not been examined in other systems, baicalein-mediated HO-1 accumulation was shown to provide cytoprotection against oxidative stress (Chen et al., 2006; Lin et al., 2007; Choi et al., 2010; Cui et al., 2015).

In A6 cells, hemin and baicalein treatment prior to the addition of 275 μM $CdCl_2$ reduced the level of accumulation of aggregated protein and aggresome-like structures compared to $CdCl_2$ alone. Furthermore, the addition of SnPP suppressed these effects, which indicated that HO-1 enzyme activity may be involved in reducing $CdCl_2$-induced proteotoxic stress. As stated earlier, cadmium-induced protein unfolding was the result of oxidative stress and interaction of cadmium ions with the protein backbone and thiol-containing residues (Galazyn-Sidorczuk et al., 2009; Tamás et al., 2014). As mentioned previously, HO-1 enzyme activity may counteract cadmium-induced oxidative stress through the production of bilirubin, an antioxidant which was shown to reduce ROS levels in mammalian cells (Fuji et al., 2010; Ziberna et al., 2015). Hemin and baicalein

may also inhibit protein aggregation directly. For example, hemin was shown to non-specifically inhibit *in vitro* amyloid fibril-type aggregation of a variety of proteins, including alpha-synuclein, alcohol dehydrogenase, catalase, gamma-s-crystallin and beta-amyloid as well as disaggregating pre-existing fibrils (Liu et al, 2014; Hayden et al., 2015; Sonavane et al., 2017). Also, baicalein was reported to inhibit the aggregation of various proteins *in vitro* including alpha-synuclein, 1SS-alpha-lacalbumin and lysozyme (Zhu et al., 2004; Bomhoff et al., 2006; Kostka et al., 2007). Also, in mouse neuroblastoma cells, baicalein treatment was found to reduce alpha-synuclein fibril formation (Jiang et al., 2010). Therefore, it is possible that hemin and baicalein may inhibit protein aggregation directly in addition to reducing ROS levels through the expression of *ho-1* genes.

In summary, this study has shown, for the first time in amphibians, that HO-1-mediated protection against $CdCl_2$ toxicity includes not only the maintenance of actin cytoskeletal and microtubular structure but also the suppression of aggregated protein and aggresome-like structures. It is likely that the primary role of HO-1 and its metabolic products, CO and biliverdin, in this situation may be to reduce $CdCl_2$-induced ROS levels. A reduction in intracellular ROS could lower the amount of unfolded and/or damaged protein and the accumulation of aggregated protein and aggresome-like structures. Given that aquatic frogs are particularly sensitive to cadmium, future studies will examine the involvement of HO-1 in counteracting cadmium-induced toxicity during early frog development and in adults.

Acknowledgements

This research was supported by a Natural Sciences and Engineering Research Council (NSERC) Discovery grant (RGPIN-2014-04376) to J.J.H. During this research J.J.H. was the recipient of a Canada Research Chair in Stress Protein Gene Research.

References

Alam, J. and Cook, J. 2007. How many transcription factors does it take to turn on the heme oxygenase-1 gene? Am. J. Respir. Cell. Mol. Biol. 36, 166-174.

Alam, J., Wicks, C., Stewart, D., Gong, P., Touchard, C., Otterbein, S., Choi, A.M.K., Burow, M.E., and Tou, J. 2000. Mechanism of heme oxygenase-1 gene activation by cadmium in MCF-7 mammary epithelial cells, role of p38 kinase and Nrf2 transcription factor. J. Biol. Chem. 275, 27694-27702.

An, H., Statsyuk, A., 2015. An inhibitor of ubiquitin conjugation and aggresome formation. Chem. Sci. 6, 5235-5245.

Balch, W.E., Morimoto, R.I., Dillin, A., Kelly, J.W. 2008. Adapting proteostasis for disease intervention. Science. 319, 916-919.

Bharadwaj, S., Hnatov, A., Ali, A., Ovsenek, N. 1998. Induction of the DNA-binding transcriptional activities of heat shock factor 1 is uncoupled in Xenopus oocytes. Biochim. Biophys. Acta 1402, 79-85.

Baranano, D.E., Rao, M., Ferris, C.D., Snyder, S.H. 2002. Biliverdin reductase: a major physiologic cytoprotectant. Proc. Natl. Acad. Sci. U.S.A. 99, 16093-16098.

Bertin, G., Averbeck, D. 2006. Cadmium: cellular effects, modification of biomolecules, modulation of DNA repair and genotoxic consequences (a review). Biochimie 88, 1549-1559.

Blechinger, S.R., Kusch, R.C., Haugo, K., Matz, C., Chivers, D.P., Krone, P.H. 2007. Brief embryonic cadmium exposure induces a stress response and cell death in the developing olfactory system followed by long-term olfactory deficits in juvenile zebrafish. Toxicol. Appl. Pharmacol. 224, 72-80.

Bolhuis, S., Richter-Landsberg, C., 2010. Effect of proteasome inhibition by MG-132 on HSP27 oligomerization, phosphorylation, and aggresome formation in the OLN-93 oligodendroglia cell line. J. Neurochem. 114, 960-971.

Bomhoff, G., Sloan, K., McLain, C., Gogol, E.P., Fisher, M.T. 2006. The effects of the flavonoid baicalein and osmolytes on the Mg 2+ accelerated aggregation/fibrillation of carboxymethylated bovine 1SS-alpha-lactalbumin. Arch. Biochem. Biophys. 453, 75-86.

Brouard, S., Otterbein, L.E., Anrather J, Tobiasch, E., Bach, F.H., Choi, A.M., Soares, M.P. 2000. Carbon monoxide generated by heme oxygenase 1 suppresses endothelial cell apoptosis. J. Exp. Med. 192, 1015-1026.

Brunt, J., Khan, S., Heikkila, J.J. 2012. Sodium arsenite and cadmium chloride induction of proteasomal inhibition and HSP accumulation in *Xenopus laevis* A6 kidney epithelial cells. Comp. Biochem. Physiol. C. Toxicol. Pharmacol. 55, 307-317.

Chen Y.C., Chow J.M., Lin C.W., Wu C.Y., Shen S.C. 2006. Baicalein inhibition of oxidative-stress-induced apoptosis via modulation of ERKs activation and induction of HO-1 gene expression in rat glioma cells C6. Toxicol. Appl. Pharmacol. 216, 263-273.

Choi, J.H., Choi, A.Y., Yoon, H., Choe, W., Yoon, K.S., Ha, J., Yeo, E.J., Kang, I. 2010. Baicalein protects HT22 murine hippocampal neuronal cells against endoplasmic reticulum stress-induced apoptosis through inhibition of reactive oxygen species production and CHOP induction. Exp. Mol. Med. 42, 811-822.

Converso, D.P., Taillé, C., Carreras, M.C., Jaitovich, A. Poderoso, J.J., Boczkowski, J. 2006. HO-1 is located in liver mitochondria and modulates mitochondrial heme content and metabolism. FASEB J. 20, 1236-1238.

Correa-Costa, M. Amano, M.T., Camara, N.O. 2012. Cytoprotection behind heme oxygenase-1 in renal diseases. World J. Nephrol. 1, 4-11.

Cui, G., Luk, S.C., Li, R.A., Chan, K.K., Lei, S.W., Wang, L., Shen, H., Leung, G.P., Lee, S.M. 2015. Cytoprotection of baicalein against oxidative stress-induced cardiomyocytes injury through the Nrf2/Keap1 pathway. J. Cardiovasc. Pharmacol. 65, 39-46.

Dey, M., Chang, A.L., Wainwright, D.A., Ahmed, A.U., Han, Y., Balyasnikova, I.V., Lesniak, M.S. 2014. Heme oxygenase-1 protects regulatory T cells from hypoxiainduced cellular stress in an experimental mouse brain tumor model. J. Neuroimmunol. 266, 33–42.

Doré, S., Takahashi, M., Ferris, C.D., Zakhary, R., Hester, L.D., Guastella, D., Snyder, S.H. 1999. Bilirubin, formed by activation of heme oxygenase-2, protects neurons against oxidative stress injury. Proc. Natl. Acad. Sci. U.S.A. 96, 2445-2450.

Faurskov, B., Bjerregaard, H. 2002. Evidence for cadmium mobilization of intracellular calcium through a divalent cation receptor in renal distal epithelial A6 cells. Pflugers Arch. 445, 40-50.

Fernando, P., Heikkila, J.J. 2000. Functional characterization of *Xenopus* small heat shock protein, Hsp30C: the carboxyl end is required for stability and chaperone activity. Cell Stress Chaperones 5, 148-159.

Fouad, A.A., Qureshi, H.A., Al-Sultan, A.I., Yacoubi, M.T., Ali AA. 2009. Protective effect of hemin against cadmium-induced testicular damage in rats. Toxicology 257, 153-60.

Fuji, M., Inoguchi, T., Sasaki, S., Maeda, Y., Zheng, J., Kobayashi, K., Takayanagi, R. 2010. Bilirubin and biliverdin protect rodents against diabetic nephropathy by downregulating NAD(P)H oxidase. Kidney. Int. 78, 905-919.

Galazyn-Sidorczuk, M., Brzoska, M.M., Jurczuk, M., Moniuszko-Jakoniuk, J., 2009. Oxidative damage to proteins and DNA in rats exposed to cadmium and/or ethanol. Chem. Biol. Interac. 180, 31-38.

Gauley. J., Young, J.T., Heikkila, J.J. 2008. Intracellular localization of the heat shock protein, HSP110, in *Xenopus laevis* A6 kidney epithelial cells. Comp. Biochem. Physiol. A Mol. Integr. Physiol. 147, 112-121.

Gottlieb, Y., Truman, M., Cohen, L.A., Leichtmann-Bardoogo, Y., Meyron-Holtz, E.G. 2012. Endoplasmic reticulum anchored heme-oxygenase 1 faces the cytosol. Haematologica 97, 1489-1493.

Gozzelino., R, Jeney, V., Soares, M.P. 2010. Mechanisms of cell protection by heme oxygenase-1. Annu. Rev. Pharmacol. Toxicol. 50, 323-354.

Hayden, E.Y., Kaur, P., Williams, T.L., Matsui, H., Yeh, S.R., Rousseau, D.L. 2015. Heme stabilization of α-Synuclein oligomers during amyloid fibril formation. Biochemistry 54, 4599-4610.

Heikkila, J.J. 2004. Regulation and function of small heat shock protein genes during amphibian development. J. Cell. Biol. Chem. 93, 672-680.

Heikkila, J.J. 2010. Heat shock protein gene expression and function in amphibian model systems. Comp. Biochem. Physiol. A. Mol. Integr. Physiol. 156, 19-33.

Heikkila, J.J. 2017. The expression and function of hsp30-like small heat shock protein genes in amphibians, birds, fish, and reptiles. Comp. Biochem. Physiol. A. Mol. Integr. Physiol. 203, 179-192.

Heikkila, J.J., Schultz, G.A., Iatrou, K., Gedamu, L. 1982. Expression of a set of fish genes following heat or metal ion exposure. J. Biol. Chem. 257, 12000-12005.

Huber, III, W.J. Scruggs, B.A., Backes, W.L. 2009. C-terminal membrane spanning region of human heme oxygenase-1 mediates a time-dependent complex formation with cytochrome P450 reductase. Biochemistry 48, 190-197.

Huot, J., Houle, F., Spitz, D.R., Landry, J. 1996. HSP27 phosphorylation-mediated resistance against actin fragmentation and cell death induced by oxidative stress. Cancer Res. 56, 273-279.

Hwang, H.W., Lee, J.R., Chou, K.Y., Suen, C.S., Hwang, M.J., Chen, C., Shieh, R.C., Chau, L.Y. 2009. Oligomerization is crucial for the stability and function of heme oxygenase-1 in the endoplasmic reticulum. J. Biol. Chem. 284, 22672–22679.

Jancsó, Z., Hermesz, E. 2015. Impact of acute arsenic and cadmium exposure on the expression of two haeme oxygenase genes and other antioxidant markers in common carp (*Cyprinus carpio*). J. Appl. Toxicol. 35, 310-8.

Jiang, M., Porat-Shliom, Y., Pei, Z., Cheng, Y., Xiang, L., Sommers, K., Li, Q., Gillardon, F., Hengerer, B., Berlinicke, C., Smith, WW., Zack, D.J., Poirier, M.A., Ross, C.A., Duan, W. 2010. Baicalein reduces E46K alpha-synuclein aggregation in vitro and protects cells against E46K alpha-synuclein toxicity in cell models of familiar Parkinsonism. J. Neurochem. 114, 419-429.

Johri, N., Jacquillet, G., Unwin, R. Heavy metal poisoning: the effects of cadmium on the kidney. Biometals 23, 783-792.

Joseph, P. 2009. Mechanisms of cadmium carcinogenesis. Toxicol. Appl. Pharmacol. 238, 272-279.

Katoh, Y., Fujimoto, M., Nakamura, K., Inouye, S., Sugahara, K., Izu, H., Nakai, A., 2004. Hsp25, a member of the Hsp30 family, promotes inclusion formation in response to stress. FEBS Lett. 565, 28-32.

Khamis, I., Heikkila, J.J. 2013. Enhanced HSP30 and HSP70 accumulation in *Xenopus* cells subjected to concurrent sodium arsenite and cadmium chloride stress. Comp. Biochem. Physiol. C. Toxicol. Pharmacol. 158, 165-172.

Khamis, I., Heikkila, J.J. 2018. Effect of isothiocyanates, BITC and PEITC, on stress protein accumulation, protein aggregation and aggresome-like structure formation in *Xenopus* A6 kidney epithelial cells. Comp. Biochem. Physiol. C Toxicol. Pharmacol. 204, 1-13.

Khan, S., Heikkila, J.J. 2014. Distinct patterns of HSP30 and HSP70 degradation in *Xenopus laevis* A6 cells recovering from thermal stress. Comp. Biochem. Physiol. A Mol. Integr. Physiol. 168, 1-10.

Khan S., Khamis I., Heikkila J.J., 2015. The small heat shock protein, HSP30, is associated with aggresome-like inclusion bodies in proteasomal inhibitor-, arsenite- and cadmium-treated *Xenopus* kidney cells. Comp. Biochem. Physiol. A. Mol. Integr. Physiol. 189, 130-140.

Koizumi, S., Gong, P., Suzuki, K.,Murata, M., 2007. Cadmium-responsive element of the human heme oxygenase-1 gene mediates heat shock factor 1-dependent transcriptional activation. J. Biol. Chem. 282, 8715–8723.

Kostka, M., Högen, T., Danzer, K.M., Levin, J., Habeck, M., Wirth, A., Wagner, R., Glabe, C.G., Finger, S., Heinzelmann, U., Garidel, P., Duan, W., Ross, C.A.,

Kretzschmar, H., Giese, A. 2008. Single particle characterization of iron-induced pore-forming alpha-synuclein oligomers. J. Biol. Chem. 283, 10992-11003.

Lang, D., Reuter, S, Buzescu, T., August, C., Heidenreich, S. 2004. Heme-induced heme oxygenase-1 (HO-1) in human monocytes inhibits apoptosis despite caspase-3 up-regulation. Int. Immunol. 17, 155-65.

Lawal, A.O., Marnewick, J.L., Ellis, E.M. 2015. Heme oxygenase-1 attenuates cadmium-induced mitochondrial-caspase 3-dependent apoptosis in human hepatoma cell line. BMC Pharmacol. Toxicol. 16, 41.

Li-Weber M. 2009. New therapeutic aspects of flavones: the anticancer properties of *Scutellaria* and its main active constituents Wogonin, Baicalein and Baicalin. Cancer Treat. Rev. 35, 57-68.

Lin, H.Y., Shen, S.C., Lin, C.W., Yang, L.Y., Chen, Y.C. 2007. Baicalein inhibition of hydrogen peroxide-induced apoptosis via ROS-dependent heme oxygenase 1 gene expression. Biochim. Biophys. Acta. 1773, 1073-1086.

Linnenbaum, M., Busker, M., Kraehling, J.R., Behrends, S. 2012. Heme oxygenase isoforms differ in their subcellular trafficking during hypoxia and are differentially modulated by cytochrome P450 reductase. PLOS ONE. 7, e35483.

Liu, Y., Carver, J.A., Ho, L.H., Elias, A.K., Musgrave, I.F., Pukala, T.L. 2014. Hemin as a generic and potent protein misfolding inhibitor. Biochem. Biophys. Res. Commun. 454, 295-300.

MacLeod, A.K., McMahon, M., Plummer, S.M., Higgins, L.G., Penning, T.M., Igarashi, K., Hayes, J.D. 2009. Characterization of the cancer chemopreventive NRF2-dependent gene battery in human keratinocytes, demonstration that the KEAP1-NRF2 pathway, and not the BACH1-NRF2 pathway, controls cytoprotection against electrophiles as well as redox-cycling compounds. Carcinogenesis 30, 1571-1580

Mendez-Armenta, M., Rios, C. 2007. Cadmium neurotoxicity. Environ. Toxicol. Pharmacol. 23, 350-358.

Miyake M., Fujimoto K., Anai S., Ohnishi, S., Nakai, Y., Inoue, T., Matsumara, Y., Tomioka, A., Ikeda, T., Okajma, E., Tanaka, N., Hirao, Y. 2010. Inhibition of heme oxygenase-1 enhances the cytotoxic effect of gemcitabine in urothelial cancer cells. Anticancer Res. 30, 2145-2152.

Morimoto, R.I. 2008. Proteotoxic stress and inducible chaperone networks in neurodegenerative disease and aging. Genes Dev. 22, 1427-1438.

Morita, T., Mitsialis, S.A., Koike, H., Liu, Y., Kourembanas, S. 1997. Carbon monoxide controls the proliferation of hypoxic smooth muscle cells. J. Biol. Chem. 272, 32804–32809.

Mouchet, F., Baudrimont, M., Gonzalez, P., Cuenot, Y., Bourdineaud, J.P., Boudou, A., Gauthier, L. 2006. Genotoxic and stress inductive potential of cadmium in *Xenopus laevis* larvae. Aquat. Toxicol. 78, 157-166.

Music, E., Khan, S., Khamis, I., Heikkila, J.J. 2014. Accumulation of heme oxygenase-1 (HSP32) in *Xenopus laevis* A6 kidney epithelial cells treated with sodium arsenite, cadmium chloride or proteasomal inhibitors. Comp. Biochem. Physiol. C. Toxicol, Pharmacol. 166, 75-87.

Namba, F., Go, H., Murphy, J.A., La, P., Yang, G., Sengupta, S., Fernando, A.P., Yohannes, M., Biswas, C., Wehrli, S.L. and Dennery, P.A. 2014. Expression level and subcellular localization of heme oxygenase-1 modulates its cytoprotective properties in response to lung injury: a mouse model. PLOS ONE. 9, e90936.

Nawaz, M., Manzi, C., Krumschnabel, G. 2005. In vitro toxicity of copper, cadmium, and chromium to isolated hepatocytes from carp, *Cyprinus carpio L*. Bull. Environ. Contam. Toxicol. 75, 652-661,

Nordberg, G. F. 2009. Historical perspectives on cadmium toxicology. Toxicol. Appl. Pharmacol. 238, 192–200.

Ogawa, K., Sun, J., Taketani, S., Nakajima, O., Nishitani, C., Sassa, S., Hayashi, N., Yamamoto, M., Shibahara, S., Fujita, H., Igarashi, K. 2001. Heme mediates derepression of Maf recognition element through direct binding to transcription repressor Bach1. EMBO J. 20, 2835-2843.

Ovelgönne, J.H., Bitorina, M., Van Wijk, R. 1995. Stressor-specific activation of heat shock genes in H35 rat hepatoma cells. Toxicol. Appl. Pharmacol. 135, 100-109.

Perrino, B.A., Chou, I.N. 1986. Role of calmodulin in cadmium-induced microtubule disassembly. Cell Biol. Int. Rep. 10, 565-573.

Platt, J.L., Nath, K.A. 1998. Heme oxygenase, protective gene or Trojan horse? Nat. Med. 12,1392-1396.

Ryter, S.W., Alam, J., and Choi, A.M. 2006. Heme oxygenase-1/carbon monoxide, from basic science to therapeutic applications. Physiol. Rev. 86, 583-650.

Sacca, P., Meiss, R., Casas, G., Mazza, O., Calvo, J.C., Navone, N., Vazquez, E. 2007. Nuclear translocation of haeme oxygenase-1 is associated to prostate cancer. Br. J. Cancer. 97, 1683–1689.

Salahudeen, A.A., Jenkins, J.K., Huang, H., Ndebele, K., Salahudeen, A.K. 2001. Overexpression of heme oxygenase protects renal tubular cells against cold storage injury: studies using hemin induction and HO-1 gene transfer. Transplantation 72, 1498-1504.

Sardana, M.K., Sassa, S., Kappas, A. 1982. Metal ion-mediated regulation of heme oxygenase induction in cultured avian liver cells. J. Biol. Chem. 257, 4806-4811

Selim, M.E., Rashed el, H.A., Aleisa, N.A., Daghestani, M.H. 2012. The protection role of heat shock protein 70 (HSP-70) in the testes of cadmium-exposed rats. Bioinformation 8, 58-64.

Shirriff, C.S., Heikkila, J.J. 2017. Characterization of cadmium chloride-induced BiP accumulation in *Xenopus laevis* A6 kidney epithelial cells. Comp. Biochem. Physiol. C. Toxicol. Pharmacol. 191, 117-128.

Sikorski, E.M., Uo, T., Morrison, R.S., Agarwal, A. 2006. Pescadillo interacts with the cadmium response element of the human heme oxygenase-1 promoter in renal epithelial cells. J. Biol. Chem. 281, 24423-30.

Søfteland, L., Holen, E., Olsvik, P.A. 2010. Toxicological application of primary hepatocyte cell cultures of Atlantic cod (*Gadus morhua*)—effects of BNF, PCDD and Cd. Comp. Biochem. Physiol. C Toxicol. Pharmacol. 151, 401-411.

Somji, S., Todd, J.H., Sens, M.A., Garrett, S.H., Sens, D.A. 2000. Expression of heat shock protein 60 in human proximal tubule cells exposed to heat, sodium arsenite and CdCl(2). Toxicol. Lett. 115, 127-136.

Sonavane, S., Haider, S.Z., Kumar, A., Ahmad, B. 2017. Hemin is able to disaggregate lysozyme amyloid fibrils into monomers. Biochim. Biophys. Acta. 1861, 1315-1325.

Srisook K., Jung, N.H., Kim, B.R., Cha, S.H., Kim, H.S., Cha, Y.N. 2005. Heme oxygenase-1-mediated partial cytoprotective effect by NO on cadmium-induced cytotoxicity in C6 rat glioma cells. Toxicol. In Vitro. 19, 31-39.

Stocker, R., Yamamoto, Y., McDonagh A.F., Glazer, A.N., Ames, B.N. 1987. Bilirubin is an antioxidant of possible physiological importance. Science. 235, 1043-1046.

Tamás, M.J., Sharma, S.K., Ibstedt, S., Jacobson, T., Christen, P. 2014. Heavy metals and metalloids as a cause for protein misfolding and aggregation. Biomolecules. 4, 252-267.

Taylor, J.P., Tanaka, F., Robitschek, J., Sandoval, C.M., Taye, A., Markovic-Plese, S., Fischbeck, K.H. 2003. Aggresomes protect cells by enhancing the degradation of toxic polyglutamine-containing protein. Hum. Mol. Genet. 12, 749-57.

Templeton, D.M., Liu, Y. 2010. Multiple roles of cadmium in cell death and survival. Chem. Biol. Interact. 188, 267-275.

Tyedmers , J., Mogk, A., Bukau, B. 2010. Cellular strategies for controlling protein aggregation. Nat. Rev. Mol. Cell Biol. 11, 777-788.

Varga, C., Laszlo, F., Fritz, P., Cavicchi, M., Lamarque, D., Horvath, K., Posa, A., Berko, A., Whittle, B.J.R. 2007. Modulation by heme and zinc protoporphyrin of colonic heme oxygenase-1 and experimental inflammatory bowel disease in the rat. Eur. J. Pharmacol. 561, 164-171.

Voellmy, R. 2004. On mechanisms that control heat shock transcription factor activity in metazoan cells. Cell Stress Chaperones 9, 122-133.

Voyer, J., Heikkila, J.J. 2008. Comparison of the effect of heat shock factor inhibitor, KNK437, on heat shock- and chemical stress-induced hsp30 gene expression in *Xenopus laevis* A6 cells. Comp. Biochem. Physiol. A Mol. Integr. Physiol. 151, 253-261.

Waisberg, M., Joseph, P., Hale, B., Beyersmann, D. 2003. Molecular and cellular mechanisms of cadmium carcinogenesis. Toxicology 192, 95–117.

Wang, Z., Chin, T.A., Templeton, D.M. 1996. Calcium-independent effects of cadmium on actin assembly in mesangial and vascular smooth muscle cells. Cell Motil. Cytoskeleton 33, 208-222.

Wong, R.J., Vreman, H.J., Shulz, S., Kalish, F.S., Pierce, N.W., Stevenson, D.K. 2011. In vitro inhibition of heme oxygenase isoenzymes by metalloporphyrins. J. Perinatol. 31, S35-S41.

Woolfson, J.P., Heikkila, J.J. 2009. Examination of cadmium-induced expression of the small heat shock protein gene, hsp30 in *Xenopus laevis* A6 kidney epithelial cells. Comp. Biochem. Physiol. A. Mol. Integr. Physiol. 152, 91-99.

Yoneya, R., Ozasa, H., Nagashima, Y., Koike, Y., Teraoka, H., Hagiwara, K., Horikawa, S. 2000. Hemin pretreatment ameliorates aspects of the nephropathy induced by mercuric chloride in the rat. Toxicol. Lett. 116, 223-229.

Yoshida, T., Sato, M. 1989. Posttranslational and direct integration of heme oxygenase into microsomes. Biochem. Biophys. Res. Commun. 163, 1086-1092.

Young, J.T., Heikkila, J.J. 2010. Proteasome inhibition induces hsp30 and hsp70 gene expression as well as the acquisition of thermotolerance in *Xenopus laevis* A6 cells. Cell Stress Chaperones 15, 323-334.

Zenke-Kawasaki, Y., Dohi, Y., Katoh, Y., Ikura, T., Ikura, M., Asahara, T., Tokunaga, F., Iwai, K., Igarashi, K. 2007. Heme induces ubiquitination and degradation of the transcription factor Bach1. Mol. Cell Biol. 27, 6962-6971.

Zhang, Z., Cui, W., Li, G., Yuan, S., Xu, D., Hoi, M.P., Lin, Z., Dou, J., Han, Y., Lee, S.M. 2012. Baicalein protects against 6-OHDA-induced neurotoxicity through activation of Keap1/Nrf2/HO-1 and involving PKCα and PI3K/AKT signaling pathways. J. Agric. Food Chem. 60, 8171-8182.

Zhu, M., Rajamani, S., Kaylor, J., Han, S., Zhouh, F., Fink, A.L. 2004. The flavanoid baicalein inhibits fibrillation of alpha-synuclein and disaggregates existing fibrils. J. Biol. Chem. 279, 26846-26857.

Ziberna, L., Martelanc, M., Franko, M., Passamonti, S. 2016. Bilirubin is an endogenous antioxidant in human vascular endothelial cells. Sci. Rep. 6, 29240. doi: 10.1038/srep29240.

Figure legends

Figure 1. Effect of $CdCl_2$ on HO-1, HSP, protein aggregation and aggresome-like structure accumulation in A6 cells. A) Cells were maintained at 22 °C (C) or treated with 25, 50, 100 or 200 μM of $CdCl_2$ (Cd) for 16 h at 22 °C. Proteins were isolated and used to generate immunoblots using anti-HO-1, anti-HSP70, anti-HSP30 and anti-actin antibodies as described in Materials and methods (representative immunoblots are shown). In densitometric analysis, the results were expressed as % mean relative density in comparison to the maximum band density obtained for each protein, which was 200 μM $CdCl_2$ for HO-1, HSP70 and HSP30. Standard error was indicated by the vertical bars. A one-way ANOVA and a Tukey's post-hoc test was used to determine significance ($p < 0.05$), as represented by an asterisk, between control cells and treated cells. These data are representative of 3 separate experiments. Immunocytochemical analysis was employed to examine the effect of $CdCl_2$ on the localization HO-1, HSP30, aggregated protein and aggresome-like structures. Cells, which were cultured on glass coverslips, were incubated in media (C) or media supplemented with 200 μM $CdCl_2$ (Cd) for 16 h at 22 °C. Nuclei and actin filaments were stained directly using DAPI (blue) and rhodamine phalloidin (red), respectively (panels B and C). HO-1 was detected with an anti-HO-1 antibody and the secondary antibody conjugate, Alexa-488 fluorophore (green; panel B). Rabbit anti-HSP30 IgG antibody and an anti-rabbit IgG antibody conjugated to an Alexa-488 fluorophore were used to detect HSP30 (green; panel C). In panel D, α-tubulin was detected using a mouse anti-α-tubulin IgG antibody and an anti-

mouse IgG antibody conjugated to an Alexa-488 fluorophore (green). Aggregated protein and aggresome-like structures were detected using Proteostat dye (red). White arrows indicate aggresome-like structures. White 10 μm scale bars are indicated in the lower right of each panel. These data are representative of 3 separate trials.

Figure 2. Effect of SnPP or ZnPP treatment on 50 μM $CdCl_2$-induced HO-1 and HSP70 accumulation. A) Cells were maintained at 22 °C (C) or treated with or without a 5 μM ZnPP or 15 μM SnPP 4 h treatment prior to supplementation with 50 μM $CdCl_2$ for 16 h at 22 °C. Immunoblot analysis of isolated proteins employed anti-HO-1, anti HSP70 and anti-actin antibodies. B) Densitometric analysis of HO-1 (black bars) and HSP70 (grey bars) accumulation. The results were expressed as % mean relative density as indicated in the legend of Figure 3. The error bars indicate standard error of the mean while the significance ($p < 0.05$) compared to control was determined by the one-way ANOVA test and Tukey's post-hoc test and represented by an asterisk. These data are representative of 3 separate experiments.

Figure 3. Effect of SnPP treatment on $CdCl_2$-induced aggregated protein and aggresome-like structure accumulation. Cells were left untreated (C) or incubated with 100 μM $CdCl_2$ (Cd) for 16 h. Also, some cells were treated for 4 h with 15 μM SnPP and then incubated with or without the addition of 100 μM $CdCl_2$ for 16 h. Actin filaments were stained directly using rhodamine phalloidin (red). α-tubulin was detected using a mouse anti-α-tubulin IgG antibody and an anti-mouse IgG antibody conjugated to an Alexa-488 fluorophore (green) while nuclei were stained with DAPI (blue). Aggregated protein and aggresome-like structures were detected using the Proteostat dye (red). White arrows

indicate the presence of aggresome-like structures. White 10 μm scale bars are indicated in the lower right of each panel. These data are representative of 3 separate trials.

Figure 4. Effect of different concentrations of hemin and baicalein on HO-1 accumulation. A) Cells were maintained at 22 °C (C) or treated with either 10, 15, 20, 25 or 30 μM of hemin or 50 μM of $CdCl_2$ for 16 h at 22 °C. In panel B, cells were incubated with 50, 100, 200 or 400 μM baicalein for 16 h at 22 °C. Proteins were isolated and used to generate immunoblots using anti-HO-1 and anti-actin antibodies as described in Materials and methods (representative immunoblots are shown). In densitometric analysis of HO-1, the results were expressed as % mean relative density in comparison to the maximum band density obtained for each protein, which were 25 μM and 200 μM for hemin and baicalein, respectively. Standard error was indicated by the vertical bars. A one-way ANOVA and a Tukey's post-hoc test was used to determine significance ($p < 0.05$), as represented by an asterisk, between control cells and treated cells. These data are representative of 3 separate experiments.

Figure 5. Effect of hemin and baicalein on localization of HO-1. Cells were cultured on glass coverslips for 16 h at 22 °C. Cells were left untreated (C) or incubated with 25 μM hemin (HM) or 200 μM baicalein (BC). HO-1 was detected with an anti-HO-1 antibody and the secondary antibody conjugate, Alexa-488 fluorophore (green). Nuclei and actin filaments were stained directly using DAPI (blue) and rhodamine phalloidin (red), respectively. White 10 μm scale bars are indicated in the lower right corner of each panel. These results are representative of at least 3 separate experiments.

Figure 6. Effect of hemin treatment on Cd-induced HO-1 localization and actin organization. Cells were left untreated (C) or incubated with 275 μM $CdCl_2$ (Cd) for 16 h

at 22 °C. In other experiments, cells were treated for 4 h with 10 μM hemin (HM) and 15 μM SnPP prior to being supplemented with 275 μM $CdCl_2$. Nuclei and actin filaments were stained directly using DAPI (blue) and rhodamine phalloidin (red), respectively. HO-1 was detected with an anti-HO-1 antibody and the secondary antibody conjugate, Alexa-488 fluorophore (green). White 10 μm scale bars are indicated in the lower right of each panel. These data are representative of 3 separate experiments.

Figure 7. Effect of baicalein treatment on Cd-induced HO-1 localization and actin organization. Cells were left untreated (C) or incubated for 16 h with 275 μM $CdCl_2$ (Cd) followed by a 4 h recovery in fresh media. In other experiments, cells were treated for 4 h with 50 μM baicalein (BC) and 15 μM SnPP before supplementation with 275 μM $CdCl_2$ followed by a 4 h recovery in fresh media. Nuclei and actin filaments were stained directly using DAPI (blue) and rhodamine phalloidin (red), respectively. HO-1 was detected with an anti-HO-1 antibody and the secondary antibody conjugate, Alexa-488 fluorophore (green). White 10 μm scale bars are indicated in the lower right of each panel. These data are representative of 3 separate trials.

Figure 8. Effect of hemin treatment on Cd-induced aggregated protein and microtubular organization. Cells were left untreated (C) or incubated with 275 μM $CdCl_2$ (Cd) for 16 h followed by a 4 h recovery in fresh media. Other treatments included incubation of cells with 10 μM hemin (HM) and 15 μM SnPP for 4 h prior to supplementation with 275 μM $CdCl_2$ for 16 h followed by a 4 h recovery in fresh media. α-tubulin was detected using a mouse anti-α-tubulin IgG antibody and an anti-mouse IgG antibody conjugated to an Alexa-488 fluorophore (green). Aggregated protein and aggresome-like structures were detected by use of the Proteostat dye (red). White arrows indicate the presence of

aggresome-like structures. White 10 μm scale bars are indicated in the lower right of each panel. These data are representative of 3 separate experiments.

Figure 9. Effect of baicalein treatment on Cd-induced aggregated protein and microtubular organization. Cells were left untreated (C) or incubated with 275 μM $CdCl_2$ (Cd) for 16 h followed by a 4 h recovery in fresh media. Other treatments included incubation of cells with 50 μM baicalein (BC) and 15 μM SnPP for 4 h prior to supplementation with 275 μM $CdCl_2$ for 16 h followed by a 4 h recovery in fresh media. α-tubulin was detected using a mouse anti-α-tubulin IgG antibody and an anti-mouse IgG antibody conjugated to an Alexa-488 fluorophore (green). Aggregated protein and aggresome-like structures were detected using the Proteostat dye (red). White arrows indicate aggresome-like structures. White 10 μm scale bars are indicated in the lower right of each panel. These data are representative of 3 separate trials.

Figure 10. Effect of hemin treatment on Cd-induced HSP30 and aggregated protein and aggresome-like structures. Cells were left untreated (C) or incubated with 275 μM $CdCl_2$ (Cd) for 16 h followed by a 4 h recovery in fresh media. Other treatments included incubation of cells with 10 μM hemin (HM) and 15 μM SnPP for 4 h prior to supplementation with 275 μM $CdCl_2$ for 16 h followed by a 4 h recovery in fresh media. Rabbit anti-HSP30 IgG antibody and an anti-rabbit IgG antibody conjugated to an Alexa-488 fluorophore were used to detect HSP30 (green). Aggregated protein and aggresome-like structures (white arrows) was detected by means of the Proteostat dye. White 10 μm scale bars are indicated in the lower right of each panel. These data are representative of 3 separate experiments.

Figure 11. Effect of baicalein treatment on Cd-induced HSP30 and aggregated protein and aggresome-like structure accumulation. Cells were left untreated (C) or incubated with 275 μM $CdCl_2$ (Cd) for 16 h followed by a 4 h recovery in fresh media. Other treatments included incubation of cells with 50 μM baicalein (BC) and 15 μM SnPP for 4 h prior to supplementation with 275 μM $CdCl_2$ for 16 h followed by a 4 h recovery in fresh media. Rabbit anti-HSP30 IgG antibody and an anti-rabbit IgG antibody conjugated to an Alexa-488 fluorophore were used to detect HSP30 (green). Aggregated protein and aggresome-like structures were detected using Proteostat dye (red). White arrows indicate aggresome-like structures. White 10 μm scale bars are indicated in the lower right of each panel. These data are representative of 3 separate trials.

Campbell and Heikkila Fig. 1.

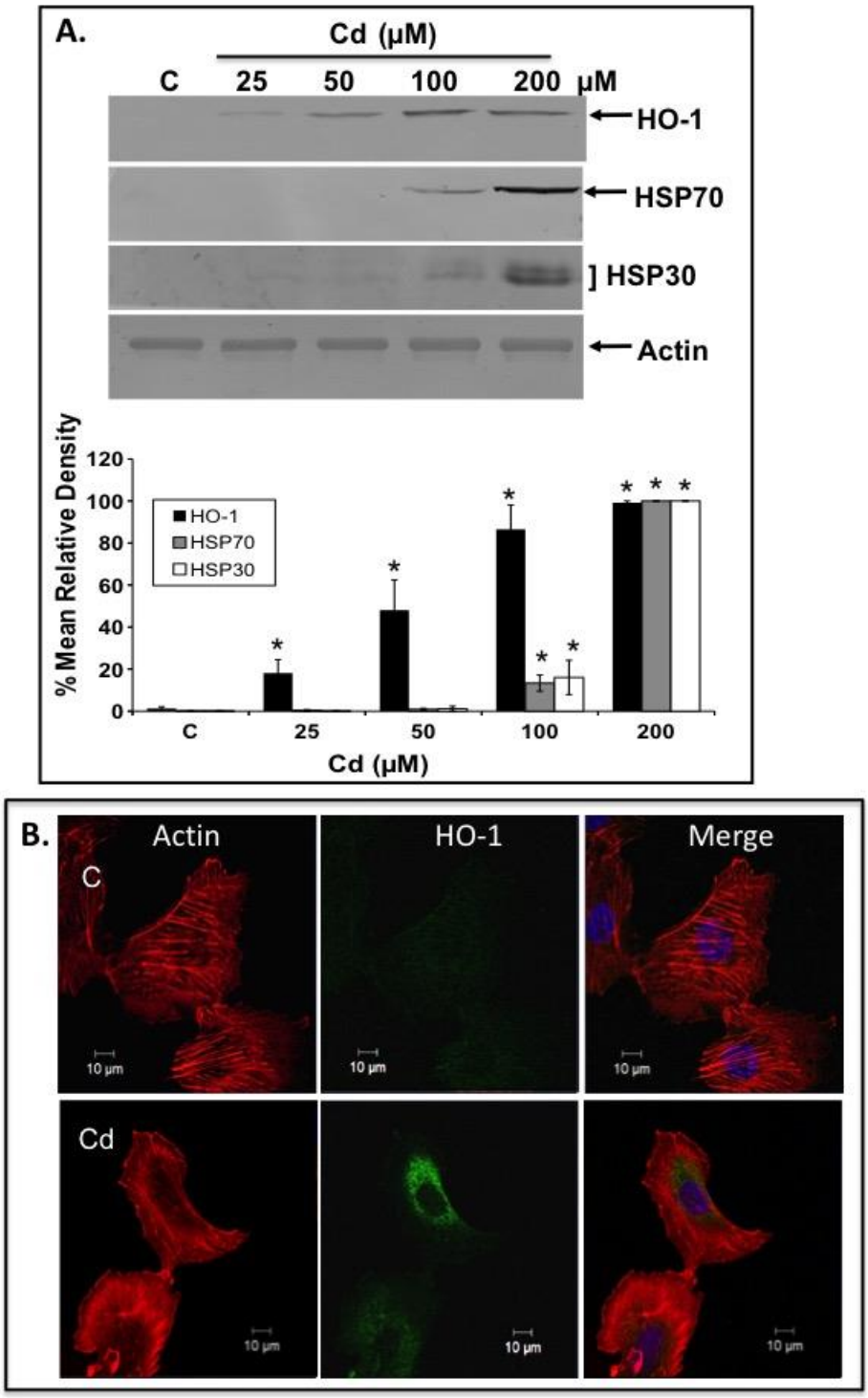

Campbell and Heikkila Fig. 1 (continued)

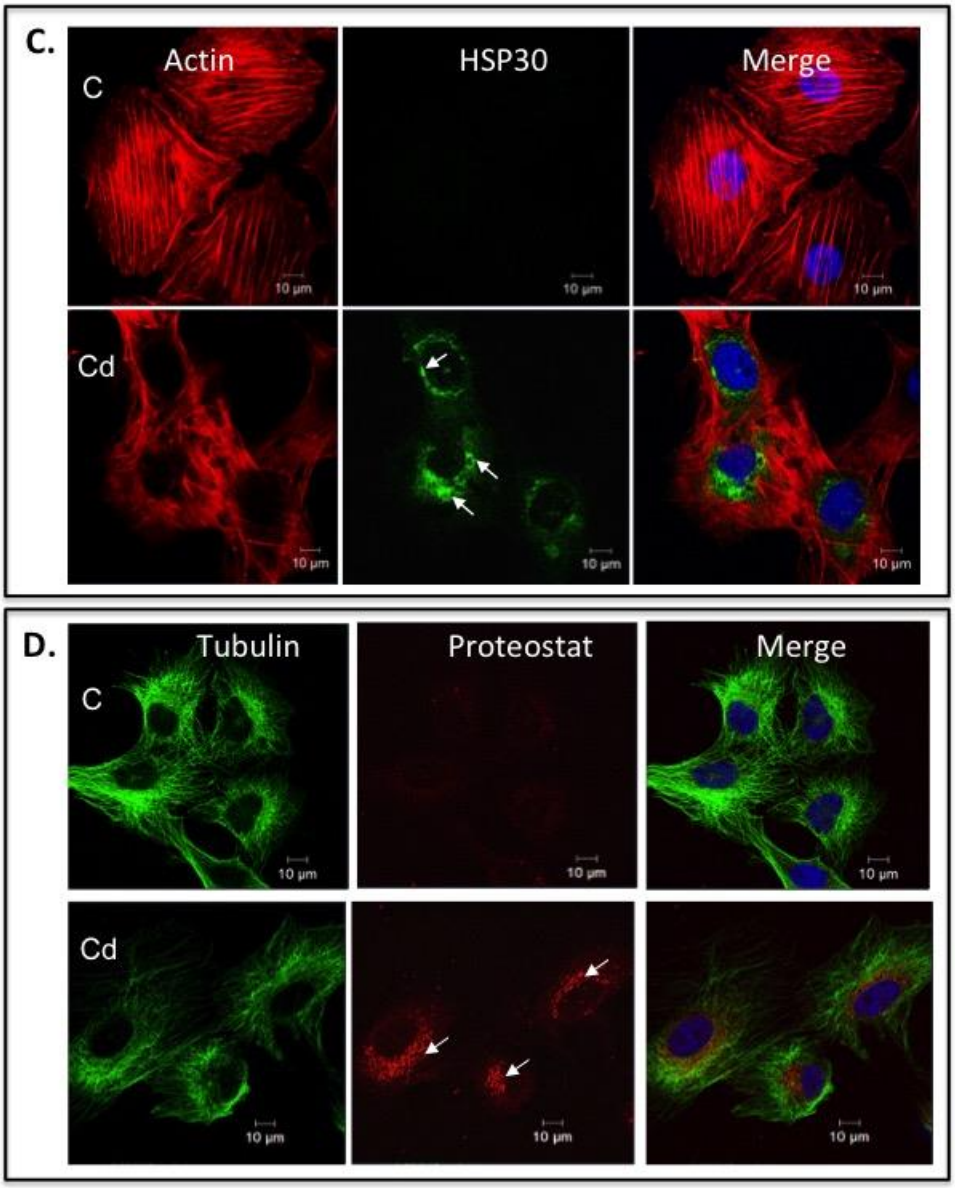

Campbell and Heikkila Fig. 2

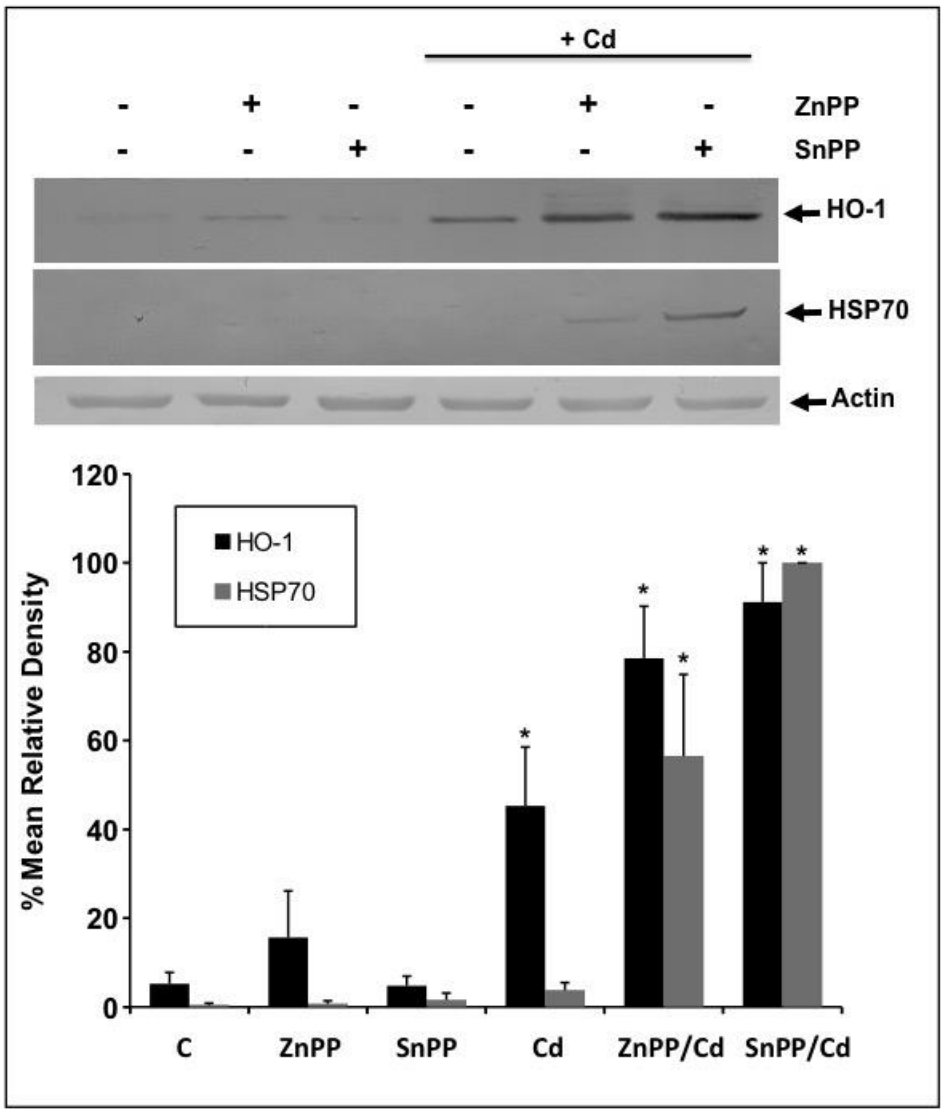

Campbell and Heikkila Fig. 3

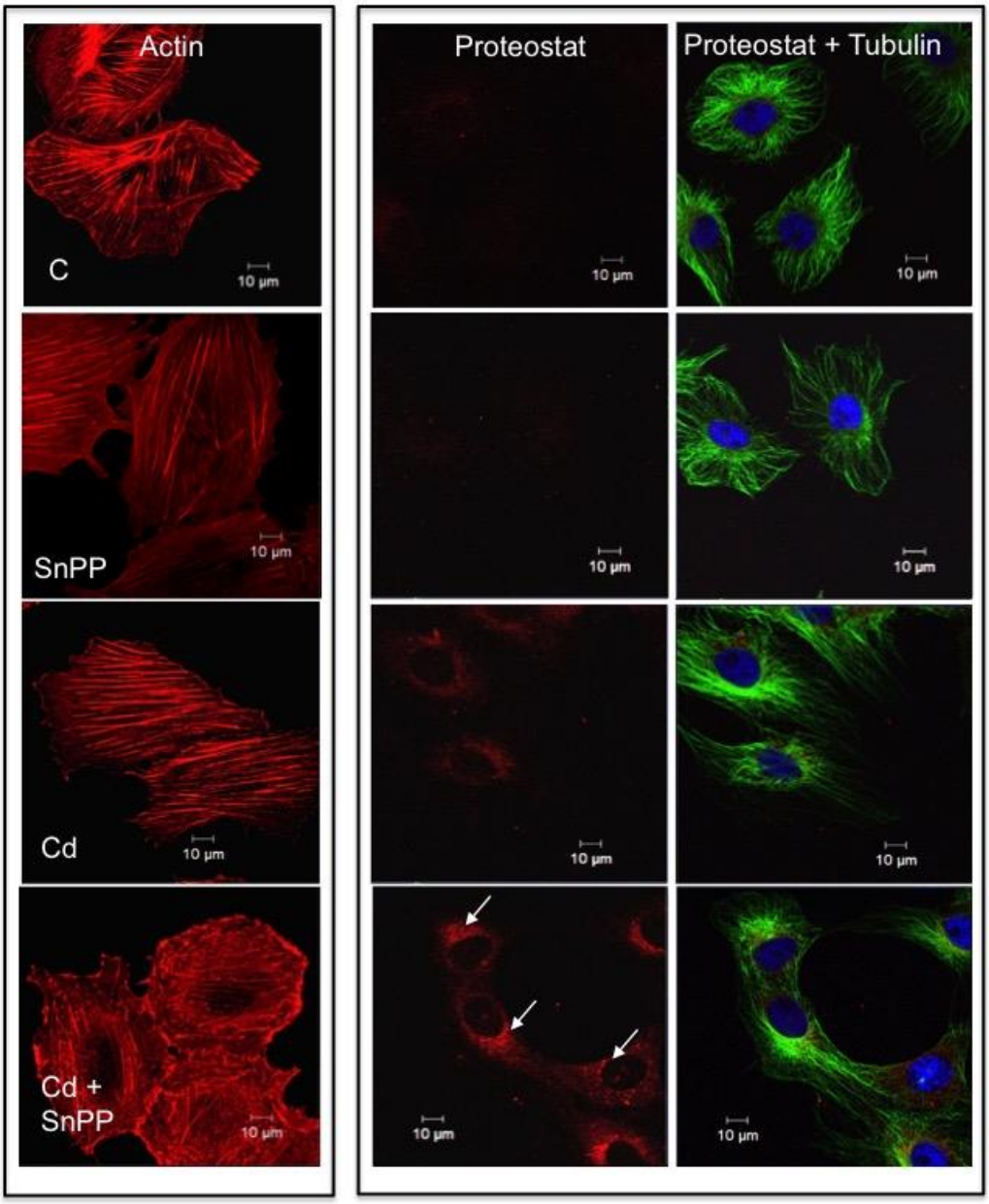

Campbell and Heikkila Fig. 4

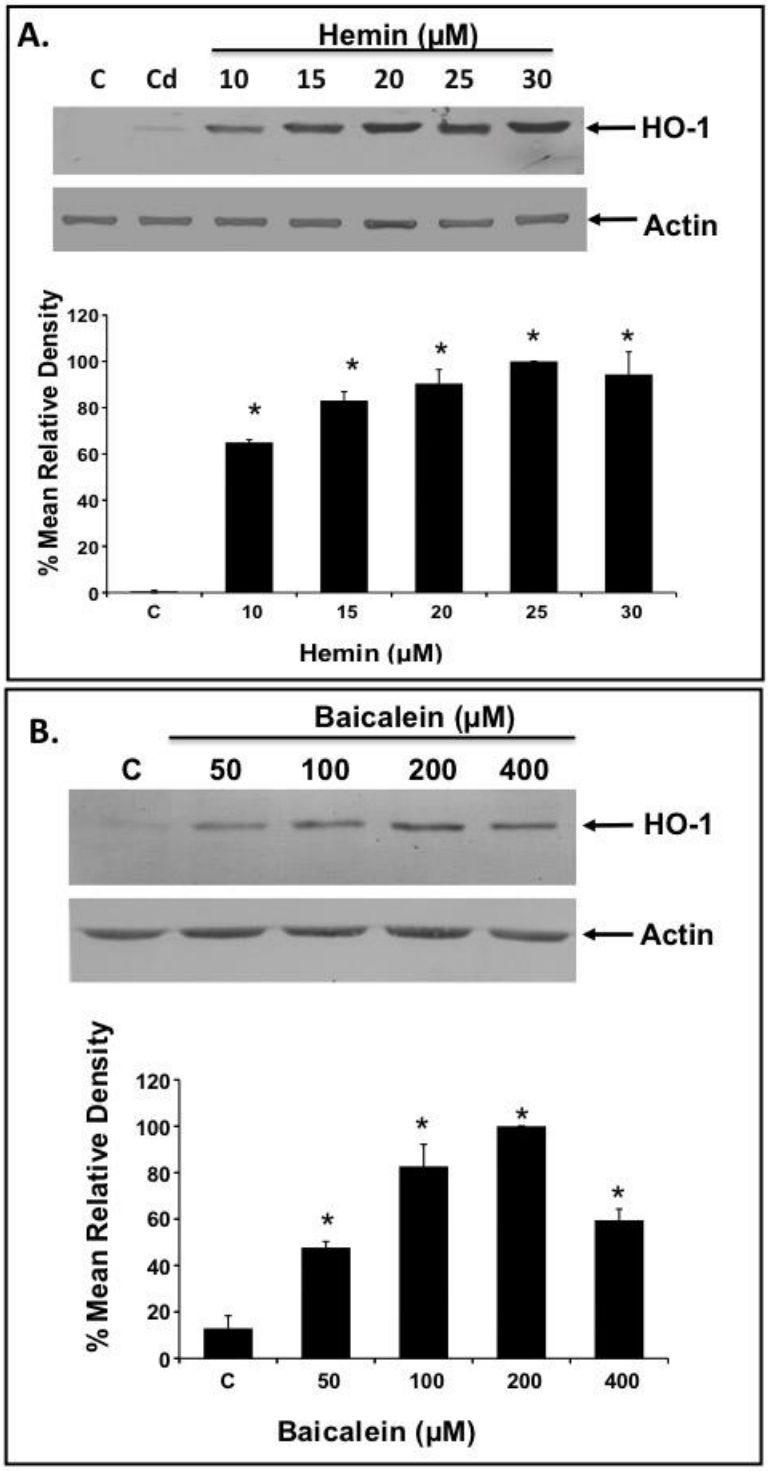

Campbell and Heikkila Fig. 5

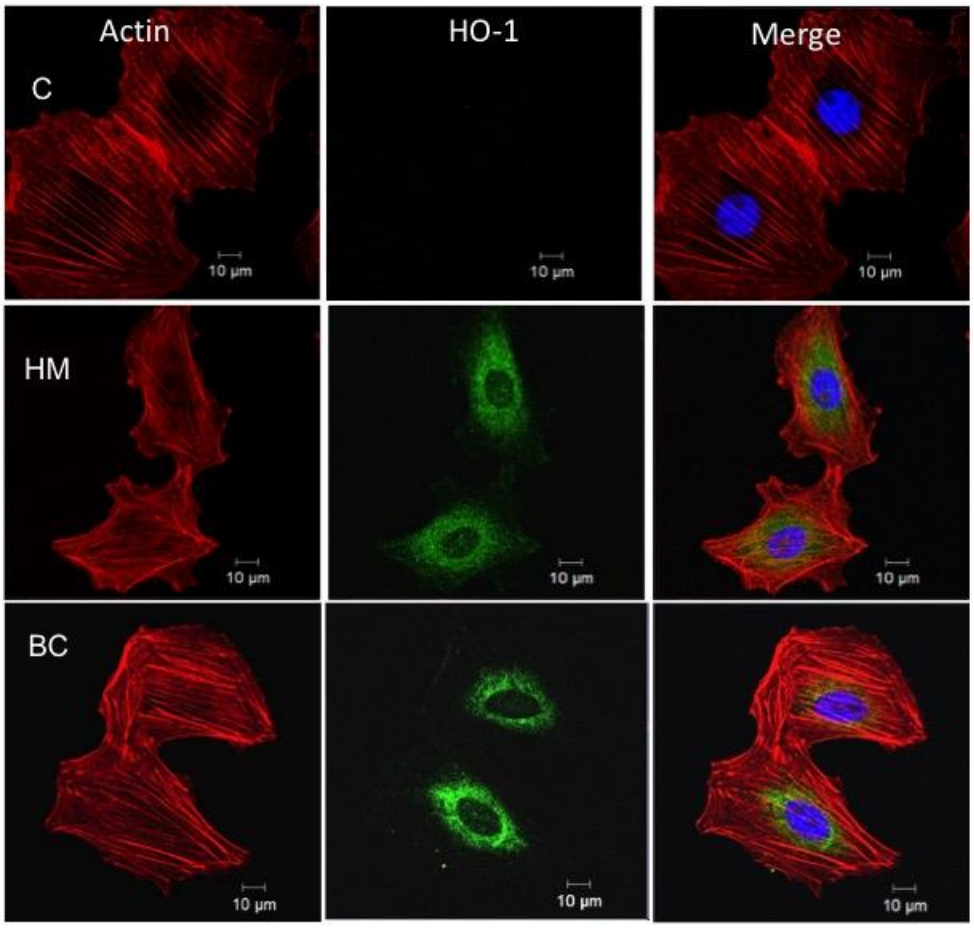

Campbell and Heikkila Fig. 6

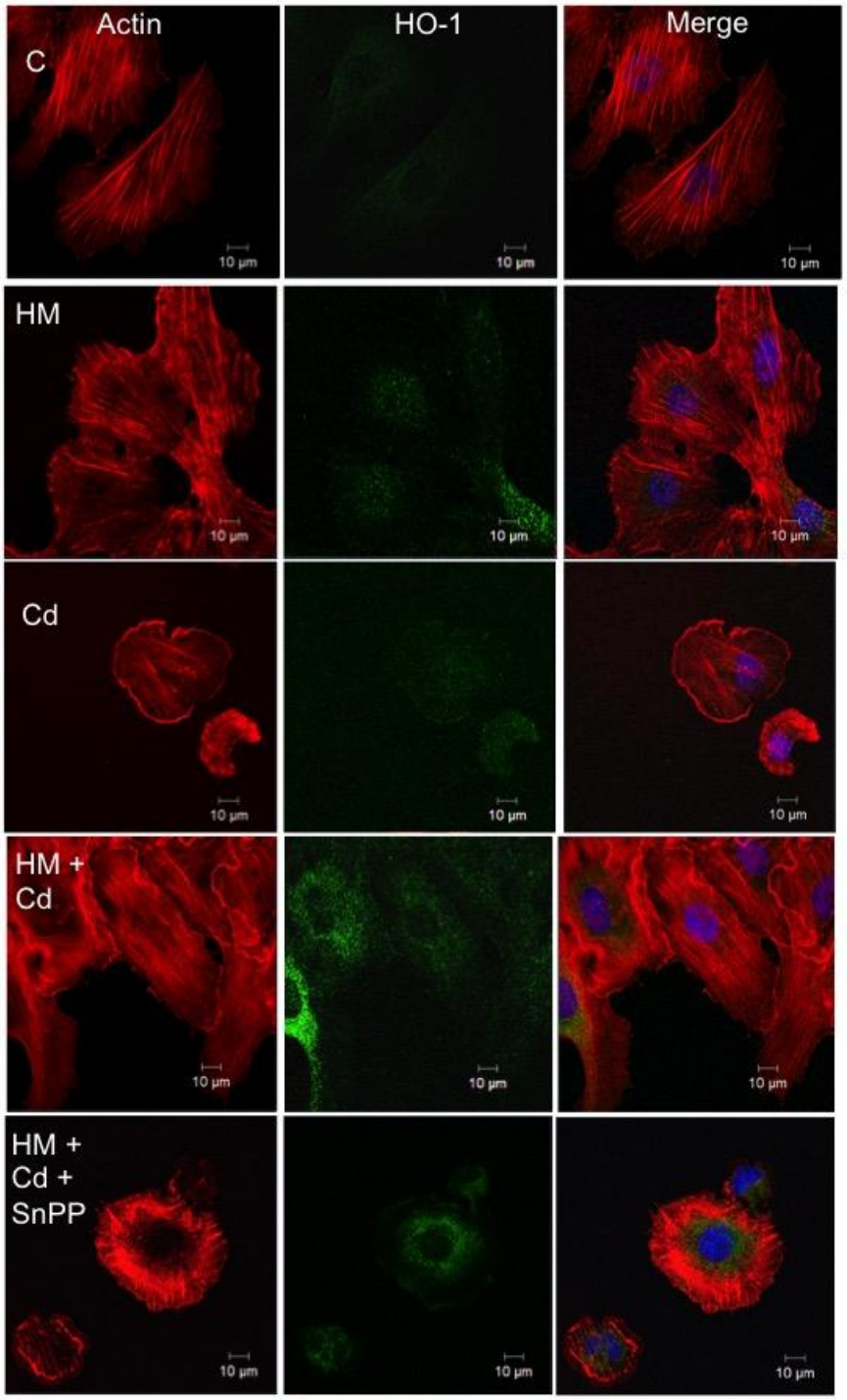

Campbell and Heikkila Fig. 7.

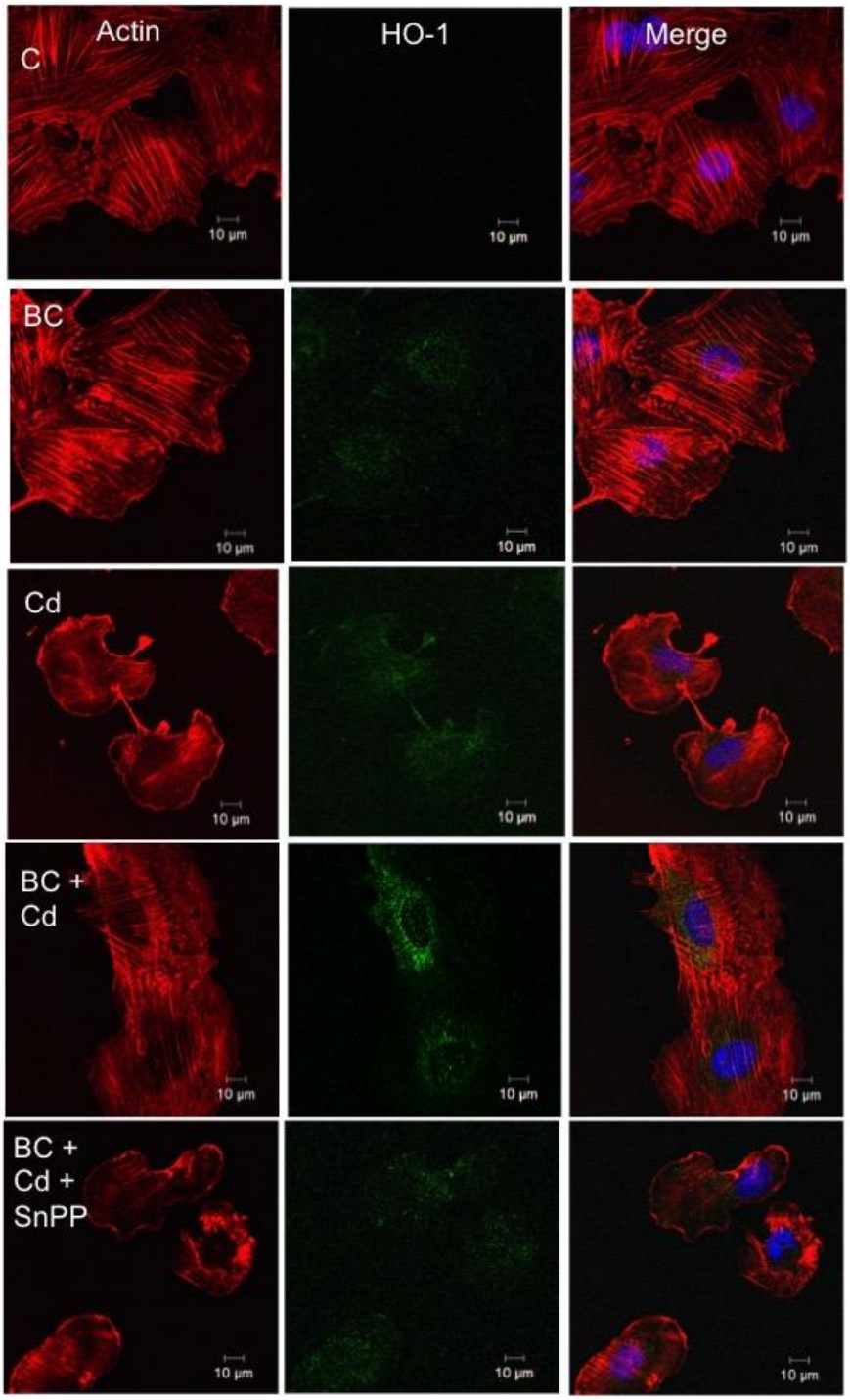

Campbell and Heikkila Fig. 8.

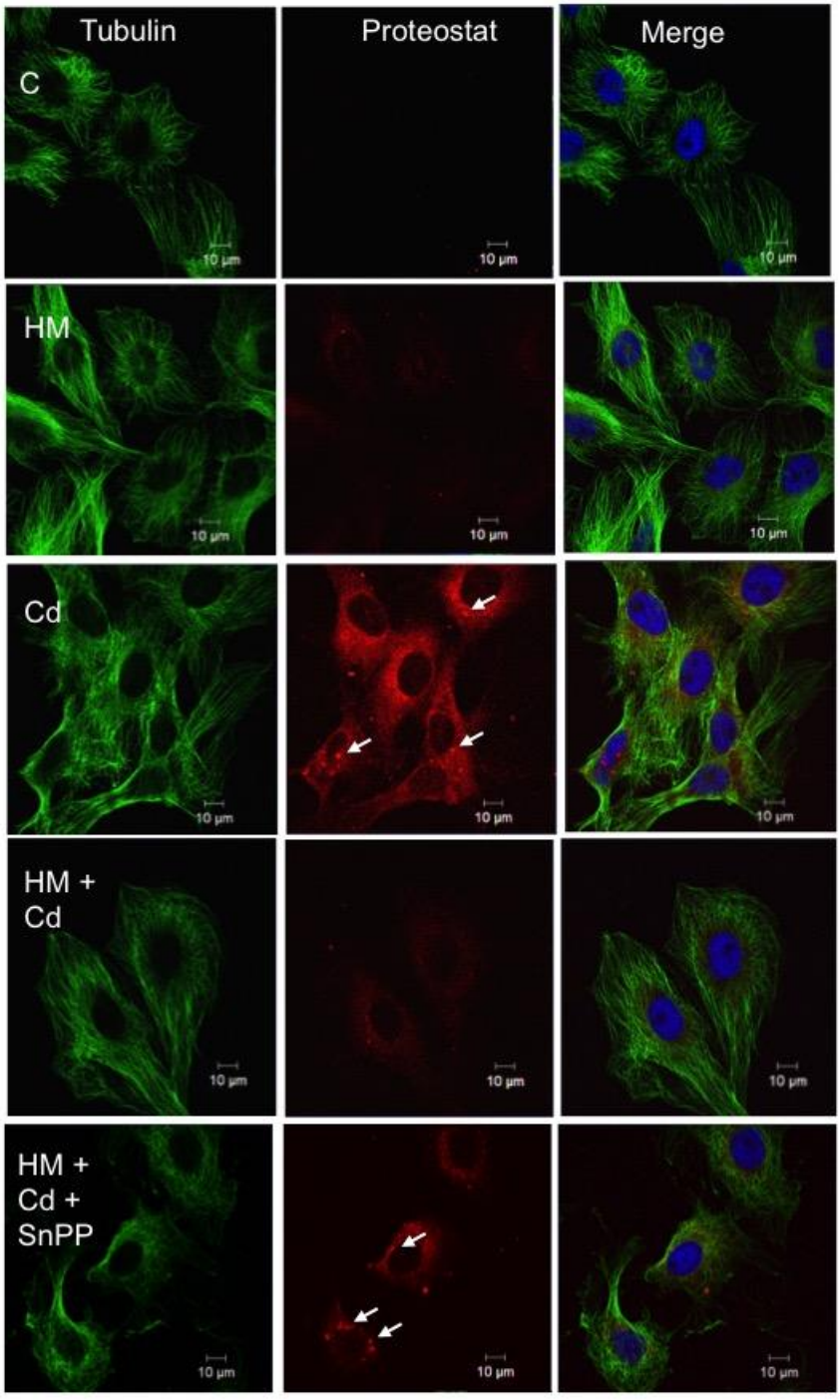

Campbell and Heikkila Fig. 9.

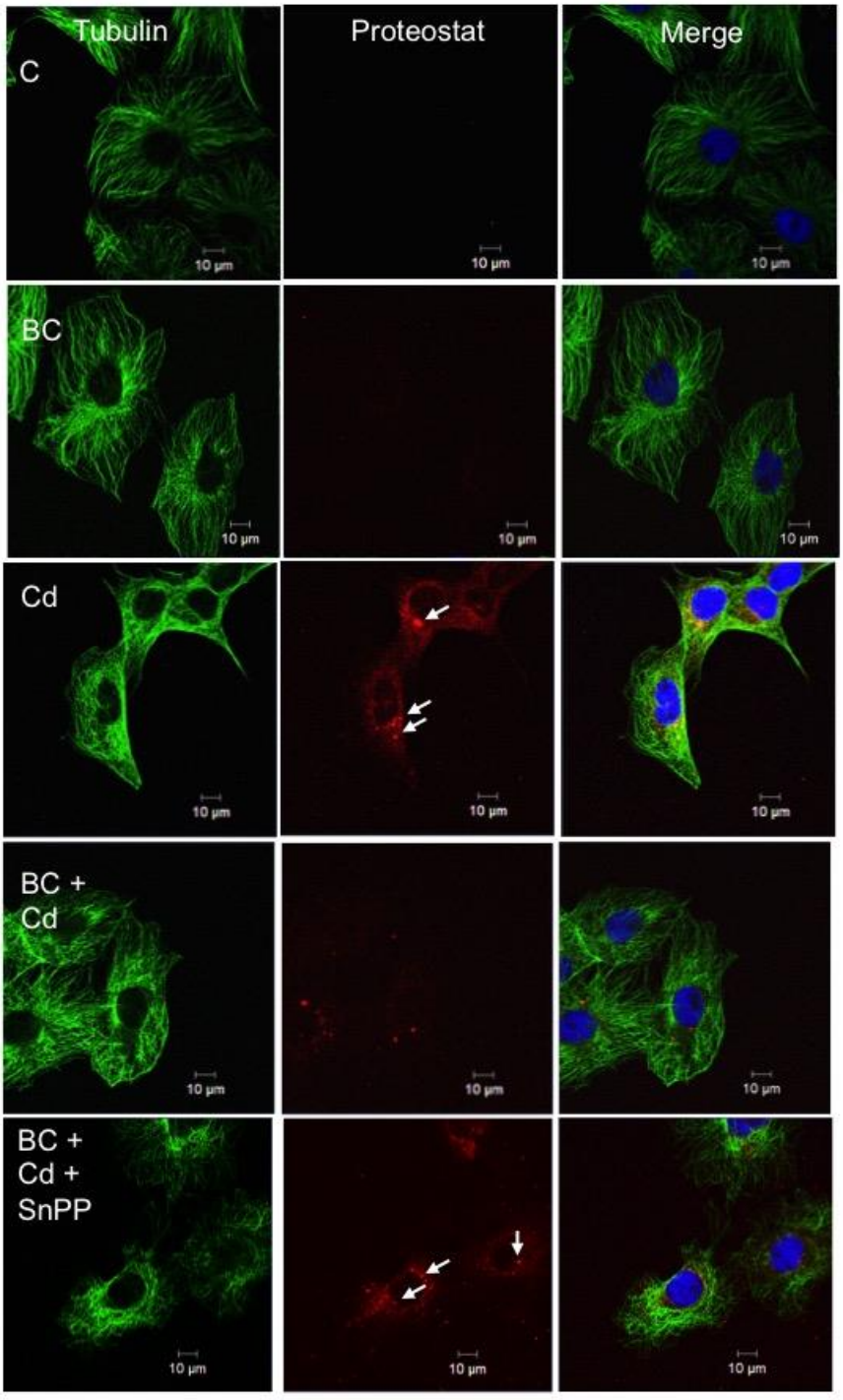

Campbell and Heikkila Fig. 10.

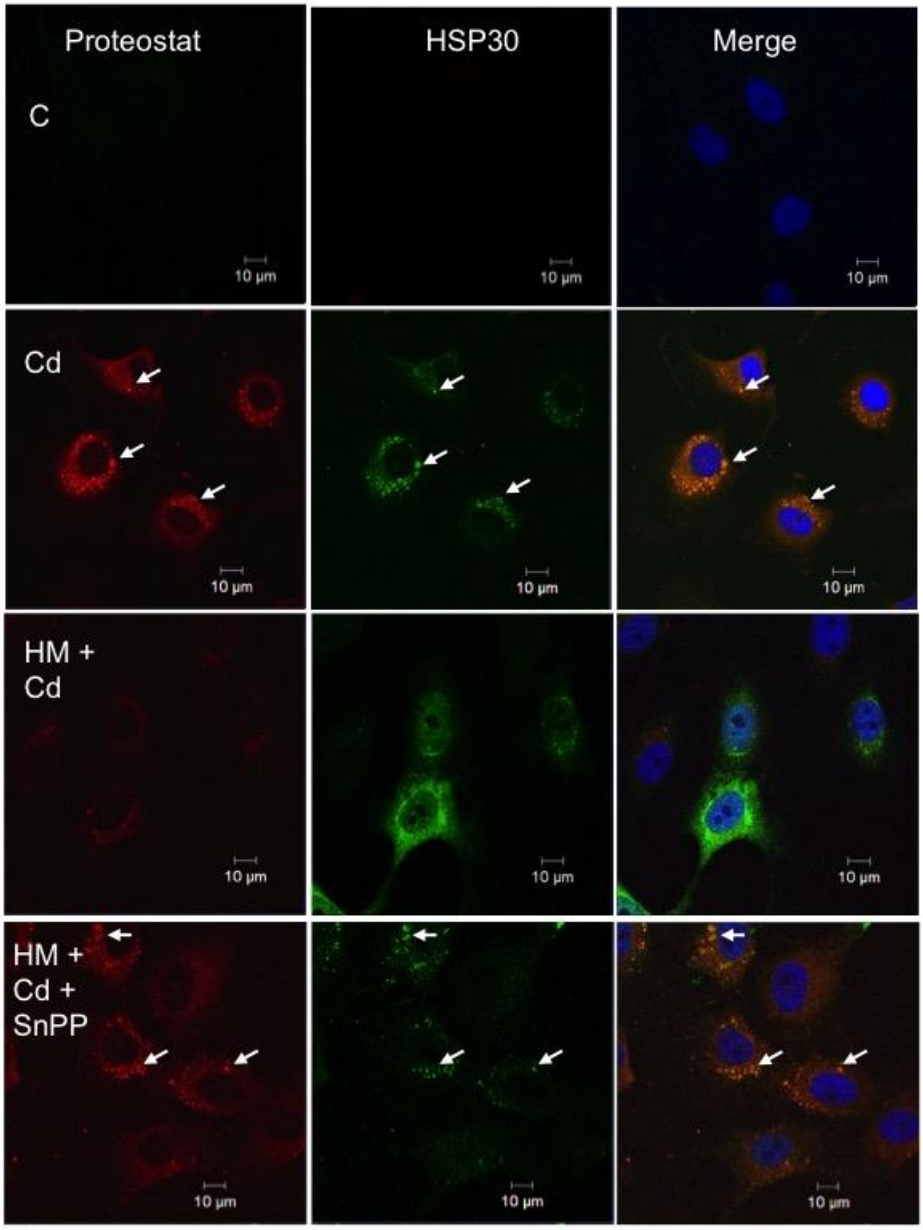

Campbell and Heikkila Fig. 11.